Environment International 208 (2026) 110080

Contents lists available at ScienceDirect

Environment International

journal homepage: www.elsevier.com/locate/envint

Full length article

Prenatal exposure to persistent organic pollutants modulates the metabolism and gut microbiota of the offspring

Santosh Lamichhane [a,b,c], Samira Salihovic [d,e], Tim Sinioja [e], Suvi M. Virtanen [f,g,h,i], Tommi Vatanen [j], Matej Orešič [c,d], Mikael Knip [c,i,j], Tuulia Hyötyläinen [e,*]

[a] Research Centre for Infections and Immunity, Institute of Biomedicine, University of Turku and Turku University Hospital, Turku, Finland
[b] Turku Clinical Microbiome Bank, Clinical Microbiology & Microbe Centre, Turku University Hospital, University of Turku University of Turku and Wellbeing Services County of Southwest Finland, Turku, Finland
[c] Turku Bioscience Centre, University of Turku and Åbo Akademi University, Turku, Finland
[d] School of Medical Sciences, Faculty of Medicine and Health, Örebro University, Örebro, Sweden
[e] School of Science and Technology, Örebro University, Sweden
[f] Department of Public Health, Finnish Institute for Health and Welfare, Helsinki, Finland
[g] Faculty of Social Sciences, Unit of Health Sciences, Tampere University, Tampere, Finland
[h] Tampere University Hospital, Wellbeing Services County of Pirkanmaa, Tampere, Finland
[i] Tampere Center for Child, Adolescent and Maternal Health Research, Tampere University and University Hospital, Tampere, Finland
[j] Faculty of Medicine, University of Helsinki, Helsinki, Finland

ARTICLE INFO

Keywords:
PCBs
POP
PFAS
Metabolomics
Gut microbiome
Early infancy

ABSTRACT

Emerging evidence suggests that environmental contaminants can influence both human metabolism and gut microbiota composition. However, the specific effects of prenatal exposure to persistent organic pollutants (POPs) on host–microbiome metabolic interactions remain incompletely understood. In this study, we investigated associations between prenatal exposure to POPs, including organochlorine pesticides, polychlorinated biphenyls (PCBs), and per- and polyfluoroalkyl substances (PFAS), and growth, metabolic profiles, and gut microbiota composition in infants at three months of age. Prenatal POP exposure was strongly associated with alterations in the infant metabolome, particularly affecting lipid metabolism and microbiota-derived metabolites. Among the POPs examined, PCBs showed the most pronounced influence on both metabolic profiles and gut microbial composition. The most affected metabolic pathways included fatty acid metabolism, bile acid transformation, and steroid hormone biosynthesis. Furthermore, prenatal POP exposure significantly altered the composition of the gut microbiome. PCB exposure was linked to reduced *Bifidobacterium bifidum* and *Lactobacillus paragasseri*, and increased *Erysipelatoclostridium ramosum*, along with disruptions in bile acid and amino acid metabolism. These findings suggest that early-life exposure to POPs can disrupt host–microbiome metabolic interactions, potentially through perturbation of lipid- and amino acid–related pathways.

1. Introduction

Due to their extensive use from the 1920s to the 1970s and their exceptionally long half-lives, PCBs (polychlorinated biphenyls) remain among the most widespread chemicals to which humans are consistently exposed (Klocke et al., 2020), alongside PFAS (per- and polyfluoroalkyl substances). Prenatal exposure to PCBs has been extensively studied, with evidence indicating detrimental effects on neurological development. These include impairments in executive functioning, processing speed, verbal abilities, and visual recognition memory in children (Boucher et al., 2009; Caspersen et al., 2016; Wilson et al., 2024). Similarly, prenatal and early-life exposure to PFAS has raised significant concerns due to associations with adverse health outcomes such as reduced kidney function, metabolic syndrome, thyroid dysfunction, and adverse pregnancy outcomes, including hypertensive disorders and low birth weight (Granum et al., 2013; Ashley-Martin et al., 2017; Fleisch et al., 2017; Starling et al., 2017; Zhou et al., 2017). The placenta has been identified as a critical target for PFAS, potentially driving peri- and postnatal effects that increase the risk of disease later in life. Indeed, exposure to multiple persistent organic pollutants (POPs) such as PFAS,

* Corresponding author.
E-mail address: tuulia.hyotylainen@oru.se (T. Hyötyläinen).

https://doi.org/10.1016/j.envint.2026.110080
Received 17 November 2025; Received in revised form 15 January 2026; Accepted 15 January 2026
Available online 21 January 2026

organochlorine (OC) pesticides and PCBs has been linked to placental DNA methylation changes, which have implications for prenatal POP (persistent organic pollutant) toxicity and their association with neonatal anthropometric measures (Ouidir et al., 2020). Prenatal exposure to POPs has in multiple studies been linked with decreased infant growth (Woods et al., 2017; Kalloo et al., 2020; Chen et al., 2024). Additionally, prenatal exposure to DDE (a DDT metabolite) and some PCBs is associated with increased BMI, waist circumference, and adiposity in children (Verhulst et al., 2009; Vafeiadi et al., 2015; Stratakis et al., 2022; Tang-Péronard et al., 2014). Prenatal and early-life exposure to PFAS—especially compounds such as perfluorooctanoic acid (PFOA) and perfluorosulfonic acid (PFOS)—has been associated with altered growth trajectories, increased adiposity, and impaired insulin regulation in children (Starling et al., 2019; Lee et al., 2021). Prenatal exposure to PFAS has also been associated with dysregulated metabolism and later progression to autoimmune diseases such as type 1 diabetes T1D) (McGlinchey et al., 2020), celiac disease (CD) (Sinisalu et al., 2020), irritable bowel disease (IBD) later in life (Agrawal et al., 2024). These findings suggest that different pollutants may exert divergent, and sometimes opposing, effects on neonatal outcomes.

While the detrimental health effects of POP exposure are well-documented, the molecular mechanisms underlying their toxicity remain poorly understood (Hoffman et al., 2023). Prenatal exposure to PCBs may involve molecular changes in maternal metabolism, with implications for placental and fetal metabolism. Emerging research has linked prenatal PCB exposure to metabolic alterations in offspring, although much of this data comes from studies conducted in adulthood (around 50 years of age). These studies report dysregulation in amino acid, energy, and glycan metabolism (Hoffman et al., 2023). Early-life (perinatal) exposure to PCB126 led to metabolic dysfunction, glucose intolerance, obesity-like phenotypes and gut microbiota alterations in adult mice, especially when combined with high–fat diet (Tian et al., 2022). Specifically, changes in liver amino acid and nucleotide metabolism as well as bile acid metabolism and increased hepatic lipogenesis were observed in adult mice after early life exposure. Exposure to POPs in mice has also shown affect cecal bacterial metabolism that is associated with significant decreases in microbial metabolic activity (Tian et al., 2020). Prenatal PFAS exposure has identified associations with metabolic changes at birth, particularly in lipid and bile acid metabolism (McGlinchey et al., 2019; Sinisalu et al., 2020). We have recently shown that early life exposure to PFAS affects fecal microbiota composition in mother-infant dyads, with data suggesting that the maternal microbiome was more strongly impacted by prenatal PFAS exposure, while only modest association with stool microbiome were observed in the infants (Lamichhane et al., 2023). These findings emphasize the need for further investigation into the distinct and overlapping mechanisms of prenatal PCB and PFAS toxicity, as well as their long-term effects on maternal and child health.

In this study, we investigated the associations between prenatal exposure to persistent organic pollutants (POPs)—including organochlorine pesticides (OCs), polychlorinated biphenyls (PCBs), and per- and polyfluoroalkyl substances (PFAS)—and growth, metabolic profiles, and gut microbiota composition in offspring at three months of age. Metabolic profiling was performed using three complementary LC-MS-based platforms, covering short-chain fatty acids, polar and semipolar metabolites, and a broad range of lipids. POP concentrations were quantified using two targeted analytical platforms. Gut microbiota composition was characterized using shotgun metagenomic sequencing, enabling high-resolution identification of microbial species.

2. Methods

2.1. Study population

This study is part of the Early Dietary Intervention and Later Signs of Beta-Cell Autoimmunity: Potential Mechanisms (EDIA) study, which is a small-scale randomized double-blind infant feeding trial comparing weaning infants onto an extensively hydrolyzed milk formula vs. a conventional, cow's milk-based formula. Pregnant women were recruited between January 2013 and February 2015 in Finland. Written informed consent was signed by the parents to permit analysis of their human leucocyte (HLA) genotype. Infants without HLA-conferred susceptibility to T1D were excluded from the intervention trial. Maternal serum samples were collected during pregnancy, and cord blood from 309 newborn infants was screened to determine their HLA genotype, as previously described (Hermann et al., 2003). Of these, 87 offspring were eligible, and 73 participated in the intervention trial. Serum samples were collected at 3, 9, and 12 months of age. Child growth (weight and length) and intestinal function, including lactulose mannitol (LM) ratio, fecal calprotectin, and fecal β-defensin levels, were also measured at given time points. The study design was recently reported (Siljander et al., 2021). Selected characteristics of the study subjects are shown in Table 1. Maternal diet during pregnancy was assessed at 35th week of pregnancy by a validated by validated, semiquantitative food frequency questionnaire (Erkkola et al., 2001) Food and individual nutrient intakes were calculated using the national food composition database, Fineli (https://fineli.fi/fineli/en/index). Fully (exclusive) breastfeeding was defined as the infant receiving in addition to breast milk only water or dietary supplements. Maternal serum samples were collected at the beginning of the third trimester and samples were also taken at delivery. Maternal exposure to persistent organic pollutants was assessed using pooled serum samples collected during the third trimester of pregnancy and at delivery. Pooling was performed to obtain sufficient sample volume for the quantification of multiple POPs and metabolomics and lipidomics analyses. Given the long biological half-lives and relatively stable serum concentrations of POPs, the pooled samples were considered to represent an integrated measure of maternal exposure during late pregnancy.

2.2. Chemicals

All solvents were HPLC grade or LC-MS grade, from Honeywell (Morris Plains, NJ, USA), Fisher Scientific (Waltham, MA, USA) or Sigma-Aldrich (St. Louis, MO, USA). Mass spectrometry grade ammonium acetate and reagent grade formic acid were also from Sigma-Aldrich. The lipid standards were from Avanti Polar Lipids Inc. (Alabaster, AL, USA). 13C-labeled PFAS internal standards (IS), 13C-labeled performance standards, and native calibration standards (perfluorocarboxylic acids (PFCAs) and perflurosulfonic acids (PFSAs)) were purchased from Wellington Laboratories (Guelph, Ontario, Canada) with purity $>$ 99%. One native performance standard, 7H-dodecafluoroheptanoic acid, was purchased from ABCR (Karlsruhe, Germany). Chenodeoxycholic acid (CDCA), Cholic acid (CA), Deoxycholic acid (DCA), Glycochenodeoxycholic acid (GCDCA), Glycocholic acid (GCA), Glycodehydrocholic acid (GDCA), Glycohyocholic acid (GHCA) were obtained from Sigma-Aldrich. Glycohyodeoxycholic acid (GHDCA). Hyocholic acid (HCA), Hyodeoxycholic acid (HDCA), Litocholic acid (LCA), alpha-Muricholic acid (αMCA), Tauro-alpha-muricholic acid (T-α-MCA), Tauro-beta-muricholic acid(T-β-MCA), Taurochenodeoxycholic acid (TCDCA), Taurocholic acid (TCA), Taurodehydrocholic acid (THCA), Taurodeoxycholic acid (TDCA), Taurohyodeoxycholic acid (THDCA), Taurolitocholic acid (TLCA), Tauro-omega-muricholic acid (TωMCA) and Tauroursodeoxycholic acid (TUDCA) were from Steraloids (Newport, RI, U.S.A). Glycodeoxycholic acid (GDCA) and ursocholic acid (UDCA) were from Fluka (Buchs, Switzerland). Glycolitocholic acid (GLCA and Glycoursodeoxycholic acid (GUDCA) were from Calbiochem (Gibbstown, NJ, U.S.A). Internal standards CA-d4, LCA-d4, UDCA-d4, CDCA-d4, DCA-d4, GCA-d4, GLCA-d4, GUDCA-d4 and GCDCA-d4 were obtained from Qmx laboratories Ltd. (Essex, UK). For quality assurance (QA), standard reference material serum SRM 1950 (for lipidomics and metabolomics) and 1957 (for PFAS and bile acids) was purchased from the National Institute of Standards and

Technology (NIST) at the US Department of Commerce (Washington, DC, USA). 2-diheptadecanoyl-sn-glycero-3-phosphoethanolamine (PE (17:0/17:0)), N-heptadecanoyl-D-erythro-sphingosylphosphorylcholine (SM(d18:1/17:0)), N-heptadecanoyl-D-erythro-sphingosine (Cer(d18:1/17:0)), 1,2-diheptadecanoyl-sn-glycero-3-phosphocholine (PC(17:0/17:0)), 1-heptadecanoyl-2-hydroxy-sn-glycero-3-phosphocholine (LPC (17:0)) and 1-palmitoyl-d31-2-oleoyl-sn-glycero-3-phosphocholine (PC (16:0/d31/18:1)), were purchased from Avanti Polar Lipids, Inc. (Alabaster, AL, USA), and, triheptadecanoylglycerol (TG(17:0/17:0/17:0)) and Cholesteryl 1-heptadecanoic acid (CE17:0) was purchased from Larodan AB (Solna, Sweden). Ultra purity water for the steroid analyses was obtained from Honeywell. Ammonium fluoride was obtained from Sigma-Aldrich.

High-purity native and isotopically labeled standards (>98% chemical purity) were purchased from three commercial suppliers: native calibration standard solution containing 14 PCB congeners (#74, #99, #105, #118, #138, #153, #156, #157, #170, #180, #189, #194, #206, #209) was purchased from Cambridge Isotope Laboratories (Andover, MA, USA). Native pesticides (HCB, *cis*-chlordane, *trans*-chlordane, *trans*-nonachlordane, and p,p′-DDE) were purchased from Dr. Ehrenstorfer GmbH (Augsburg, Germany). 13C-labeled PCBs (#70, #101, #105, #118, #138, #153, #156, #170, #180, #194, #206, #209), 13C-labeled pesticides (HCB and p,p′-DDE) as well as 13C-labeled recovery standards (PCBs #81, #114, and #178), were obtained from Wellington Laboratories (Guelph, Ontario, Canada). The individual standards or mixtures were accompanied by certificates of analysis with lot-specific information on purity, concentration, and recommended storage conditions to ensure traceability and reliable quantification and safety data sheets for safe handling.

2.3. Analysis of persistent organic pollutants

The sample preparation method used for extraction of persistent organic pollutants from plasma was previously described (Salihovic et al., 2012; Stubleski et al., 2018). Briefly, serum samples were spiked with 13C-labeled internal standard mixture that comprised the following PCBs: 70, 101, 105, 118, 138, 153, 156, 170, 180, 194, 206 and 209 together with 13C-labled OCDD and PBDE 47. Recovery standards were PCBs 81, 114 and 178. Next, the samples were diluted in protein precipitating solutions of 9 mM sulfuric acid (Merck, Darmstadt, Germany) and 20% (v/v) acetonitrile (Fisher Scientific, Leicestershire, UK) were transferred to an Oasis HLB 96-well plate (Waters Corporation, Milford, Massachusetts, USA). 40% (v/v) methanol (Honeywell Riedel-de Haën, Steinheim, Germany) solution in High-performance liquid chromatography (HPLC)-grade water (Fisher Scientific, Leicestershire, UK) was used to rinse the plate before the plate was dried and analytes were eluted with a 1:1 dichloromethane:hexane (Honeywell Riedel-de Haën, Steinheim, Germany and Merck, Darmstadt, Germany respectively) solution. Sulfuric acid modified silica (Sigma Aldrich/Supelco) and sodium sulfate (Sigma Aldrich/Supelco,) were used for lipid degradation and water removal from the sample extracts. Sample extracts were placed evaporated overnight with 20 μL tetradecane. Instrumental analysis was performed with an atmospheric pressure gas chromatograph (Agilent Technologies) coupled to a Xevo TQS tandem mass spectrometer (Waters Corporation, Milford, Massachusetts, USA) operating in positive atmospheric-pressure chemical ionization. Splitless injection was used to inject 2 μL of the final extract of sample onto a DB-5MS capillary column (Agilent Technologies, Santa Clara, California, USA). Isotope dilution methodology was used with a 13C-labeled internal standards standard to ensure accurate quantification of the targeted analytes. Procedural blanks, instrument blanks, in-house reference plasma, and Standard Reference Material from the National Institute for Standards and Technology (NIST) 1957 were analyzed with each batch of samples and the obtained results were compared with certified values. The results agreed well with the reference values.

PFAS analyses were performed as previously as described in (McGlinchey, Sinioja et al., 2019). Shortly, 450 μL acetonitrile with 1% formic acid, and internal standards were added to 150 μL serum and samples subsequently treated with Ostro Protein Precipitation & Phospholipid Removal 96-well plate (Waters Corporation, Milford, USA). PFAS analysis was performed using automated column-switching ultra-performance liquid chromatography coupled with tandem mass spectrometry (UPLC-MS/MS; Waters, Milford, USA) on an ACQUITY BEH C18 column (2.1 mm × 100 mm, 1.7 μm). A gradient elution was applied using 30% methanol in 2 mM NH_4Ac (aqueous phase) and 2 mM NH_4Ac in methanol (organic phase), at a flow rate of 0.3 mL/min. Quantitative analysis of the selected analytes was performed using the isotope dilution method; all standards (i.e., internal standards, recovery standards, and native calibration standards) were purchased from Wellington Laboratories (Guelph, Ontario, Canada). The method's detection limits ranged between 0.02–0.19 ng/mL, depending on the analyte. NIST SRM 1957 reference serum as well as in-house pooled plasma samples were used in quality control, and the results agreed well with the reference values.

2.4. Analysis of SCFA, lipids, polar and semipolar metabolites by UHPLC-QTOFMS

All samples were randomized before sample preparation and analysis. Three extraction methods described below were applied, the first one for extraction of bile acids, PFAS and other semipolar compounds, the second one for extraction of lipids and the third one for SCFAs. Three methods using an ultra-high-performance liquid chromatography quadrupole time-of-flight mass spectrometry (UHPLC-QTOFMS) were used for the analysis (Table 2), namely one method for comprehensive profiling of polar and semipolar metabolites, one method for comprehensive profiling of lipids, and the third method for target analysis of SCFA. Briefly, the UHPLC system used in this work was a 1290 Infinity II system from Agilent Technologies. The system was equipped with a multi sampler (maintained at 10 °C), a quaternary solvent manager and a column thermostat (maintained at 50 °C), and the QTOFMS was equipped with dual ESI ionization source. For the steroid analysis, a Sciex Exion LC system equipped with two binary pumps, an autosampler (maintained at 10 °C) and a column oven (maintained at 35 °C) was connected to a Sciex 7500 triple quadrupole mass spectrometer. SciexOS 3.1 was used data acquisition (Table 2). MassHunter B.06.01 (Agilent Technologies) was used for all data acquisition.

2.4.1. Polar and semipolar metabolites

For the analysis of bile acids, PFAS and polar metabolites, a combined target-non-target method for the analysis of semipolar metabolites and pollutants was applied. 40 μl of sample was extracted with 400 μL of cold MeOH/H_2O containing the internal standard mixture (Valine-d8, Glutamic acid-d5, Succinic acid-d4, Heptadecanoic acid, Lactic acid-d3, Citric acid-d4. 3-Hydroxybutyric acid-d4, Arginine-d7, Tryptophan-d5, Glutamine-d5, 1-D4-cholic acid, 1-D4-deoxycholic acid, 1-D4- chenodeoxycholic acid,1-D4-glyco cholic acid,1-D4-glycochenodeoxycholic acid,1-D4-glycolithocholic acid,1-D4-glycoursocholic acid,1-D4-lithocholic acid, 1-D4-taurocholic acid, 1-D4-ursocholic acid, PFOA-13C8, PFNA-13C5, PFUndA-13C7, PFHxS-13C3 and PFOS-13C8). The tube was vortexed and ultrasonicated for 3 min, followed by centrifugation (10000 rpm, 5 min). After centrifuging, 350 μl of the upper layer of the solution was transferred to the LC vial and evaporated under the nitrogen gas to the dryness. After drying, the sample was reconstituted into 60 μl of MeOH:H_2O (70:30).

Quantitation was done using 6-point calibration (PFOA c = 3.75–120 ng/mL, bile acids c = 20–640 ng/mL, polar metabolites c = 0.1 to 80 μg/mL). Quantification of other bile acids was done using the following compounds: CDCA, CA, DCA, GCDCA, GCA, GDCA, GDCA, GHCA, GHDCA, GLCA, GUDCA, HCA, HDCA, LCA, αMCA, T-α-MCA, T-β-MCA, TCDCA, TCA, THCA, TDCA, THDCA, TLCA, TωMCA and TDCA. Polar metabolites were quantified using alanine, citric acid, fumaric

acid, glutamic acid, glycine, lactic acid, malic acid, 2-hydroxybutyric acid, 3-hydroxybutyric acid, linoleic acid, oleic acid, palmitic acid, stearic acid, cholesterol, fructose, glutamine, indole-3-propionic acid, isoleucine, leucine, proline, succinic acid, valine, asparagine, aspartic acid, arachidonic acid, glycerol-3-phosphate, lysine, methionine, ornithine, phenylalanine, serine and threonine.

Standard solutions extracted blanks (n = 3), pooled QC samples (n = 9, an aliquot of each sample pooled), in-house serum QC and NIST CRM 1950 (human plasma) were analysed together with the samples for quality control. Identification was performed using an in-house library (*m/z*, MS/MS, and retention times) built from analyses of authentic standard.

2.4.2. Lipidomics

For lipidomics the samples were extracted using a modified version of the previously-published Folch procedure (Sen et al, 2022). In short, 10 μL of 0.9% NaCl and, 120 μL of $CHCl_3$:MeOH (2:1, v/v) containing the internal standards (c = 2.5 μg/mL) was added to 10 μL of sample. The standard solution contained the following compounds: PE(17:0/17:0), SM(d18:1/17:0), NCer(d18:1/17:0), PC(17:0/17:0), LPC(17:0), Cer (d18:1/17:0), CE(17:0), PC(16:0/d31/18:1) and TG(17:0/17:0/17:0). The samples were vortex mixed, incubated on ice for 30 min and then centrifuged (9400 × g, 3 min). 60 μL from the lower layer of each sample was then transferred to a glass vial with an insert and 60 μL of $CHCl_3$: MeOH (2:1, v/v) was added to each sample. The samples were stored at −80 °C until analysis.

Calibration curves using 1-hexadecyl-2-(9Z-octadecenoyl)-sn-glycero-3-phosphocholine (PC(16:0e/18:1(9Z))), 1-(1Z-octadecenyl)-2-(9Z-octadecenoyl)-sn-glycero-3-phosphocholine (PC(18:0p/18:1(9Z))), 1-stearoyl-2-hydroxy-sn-glycero-3-phosphocholine (LPC(18:0)), 1-oleoyl-2-hydroxy-sn-glycero-3-phosphocholine (LPC(18:1)), 1-palmitoyl-2-oleoyl-sn-glycero-3-phosphoethanolamine (PE(16:0/18:1)), 1-(1Z-octadecenyl)-2-docosahexaenoyl-sn-glycero-3-phosphocholine (PC(18:0p/22:6)) and 1-stearoyl-2-linoleoyl-sn-glycerol (DG(18:0/18:2)), 1-(9Z-octadecenoyl)-sn-glycero-3-phosphoethanolamine (LPE(18:1)), N-(9Z-octadecenoyl)-sphinganine (Cer(d18:0/18:1(9Z))), 1-hexadecyl-2-(9Z-octadecenoyl)-sn-glycero-3-phosphoethanolamine (PE(16:0/18:1)) from Avanti Polar Lipids, 1-Palmitoyl-2-Hydroxy-sn-Glycero-3-Phosphatidylcholine (LPC(16:0)), 1,2,3 trihexadecanoalglycerol (TG(16:0/16:0/16:0)), 1,2,3-trioctadecanoylglycerol (TG(18:0/18:0/18:)) and 3β-hydroxy-5-cholestene-3-stearate (ChoE(18:0)), 3β-Hydroxy-5-cholestene-3-linoleate (ChoE(18:2)) from Larodan, were prepared to the following concentration levels: 100, 500, 1000, 1500, 2000 and 5000 ng/mL (in $CHCl_3$:MeOH, 2:1, v/v) including 1250 ng/mL of each internal standard.

Standard solutions, extracted blanks (n = 6), pooled QC samples (n = 3, an aliquot of each sample pooled), in-house serum QC and NIST CRM 1950 (human plasma) were analysed together with the samples for quality control. Identification was done based on in-house library (mz, MS/MS, retention times).

2.4.3. SCFA and other polar metabolites

The analysis of SCFAs and other polar metabolites was conducted using UHPLC-qToF-MS after applying the 3-nitrophenylhydrazin (3-NPH) derivatization method, as previously described (Dei Cas et al., 2020) but with compound coverage expanded. Briefly, 50 μL of the serum was mixed with cold methanol (90 μL) containing the internal standards (IS, 10 μg/mL each) aceticacid-d_4, butyric acid-d8 and propionic acid-d2. The extract was ultrasonicated (5 min), then centrifuged (10000 g, 5 min, 4 °C) and supernatant was transferred (100 μL) to an LC vial. For derivatization, the sample was mixed with 50 mM 3-NPH (25 μL), 50 mM N-ethylcarbodiimide (EDC, 25 μL), and 7% pyridine (25 μL). Following an incubation period of 1 h, the derivatization reaction was stopped by adding 0.2% formic acid, and the sample was immediately subjected to UHPLC-qToF-MS analysis (Table 2).

2.5. Data preprocessing for metabolomics and lipidomic analyses

Mass spectrometry data processing was performed using the open-source software package MZmine 4.08 (Pluskal et al., 2010; Tito Damiani 2024). The following steps were applied in this processing: (1) Crop filtering with a *m/z* range of 350 – 1200 *m/z* and an RT range of 2.0 to 12 min, (2) Mass detection with a noise level of 750, (3) Chromatogram builder with a minimum time span of 0.08 min, minimum height of 1000 and a *m/z* tolerance of 0.006 *m/z* or 10.0 ppm, (4) Chromatogram deconvolution using the local minimum search algorithm with a 70% chromatographic threshold, 0.05 min minimum RT range, 5% minimum relative height, 1200 minimum absolute height, a minimum ration of peak top/edge of 1.2 and a peak duration range of 0.08–5.0, (5), Isotopic peak grouper with a *m/z* tolerance of 5.0 ppm, RT tolerance of 0.05 min, maximum charge of 2 and with the most intense isotope set as the representative isotope, (6) Join aligner with a *m/z* tolerance of 0.009 or 10.0 ppm and a weight for of 2, a RT tolerance of 0.1 min and a weight of 1 and with no requirement of charge state or ID and no comparison of isotope pattern, (7) Peak list row filter with a minimum of 10% of the samples, (8) Gap filling using the same RT and *m/z* range gap filler algorithm with an *m/z* tolerance of 0.009 *m/z* or 11.0 ppm, (9) Identification of lipids using a custom database search with an *m/z* tolerance of 0.009 *m/z* or 10.0 ppm and a RT tolerance of 0.1 min, and (10) Normalization using internal standards: Lipids: PE(17:0/17:0), SM (d18:1/17:0), Cer(d18:1/17:0), LPC(17:0), TG(17:0/17:0/17:0) and PC (16:0/d30/18:1)) for identified lipids and closest ISTD for the unknown lipids followed by calculation of the concentrations based on lipid-class concentration curves. For polar and semipolar metabolites, the following ISTDs were used Valine-d8, Glutamic acid-d5, Succinic acid-d4, Heptadecanoic acid, Lactic acid-d3, Citric acid-d4. 3-Hydroxybutyric acid-d4, Arginine-d7, Tryptophan-d5, Glutamine-d5, 1-D4-CA,1-D4-CDCA,1-D4-CDCA,1-D4-GCA,1-D4-GCDCA,1-D4-GLCA,1-D4-GUDCA,1-D4-LCA,1-D4-TCA, 1-D4-UDCA.

For data filtering, we have removed compounds that were present in blank samples (peak area < 5 times that of blank) and compounds that had a relative standard deviation (RSD) > 30% in the pooled quality control samples. MS/MS data was generated for the pooled quality control samples using auto MS/MS mode.

2.6. QC/QA for metabolomics and lipidomic and POP analyses

To evaluate the robustness of the method, relative standard deviations were calculated for the pooled samples, both for lipidomics as well as for polar metabolites. The pooled sample were prepared by taking an aliquot (10 μl) of each extract, separately for lipidomic and polar metabolite methods, and pooling them, and aliquoting the pool into three separate vials. For lipidomics, the RSD was on average 10.8% for identified metabolites and 14.6% for all compounds, among the identified compounds, 55% had an RSD below 10%. For polar and semipolar metabolites, the RSD was on average 9.1% for identified metabolites and 13.3% for all compounds, among the identified compounds, 67% had an RSD below 10%.

2.7. Stool microbiome analysis

We adapted the method as described earlier from here (Vatanen et al., 2022). Infant stool samples were collected by the mothers at home and stored in the household freezer (−20°C) until the next visit to the study centre. The samples were then shipped on dry ice to the EDIA Core Laboratory in Helsinki, where the samples were stored at − 80°C until shipping to Tampere University for DNA extraction. DNA extractions from 0.2 g of stool were carried out using the vacuum protocol of PowerSoil DNA Isolation Kit (MoBio Laboratories, Inc., Carlsbad, CA, USA) according to the manufacturer's standard protocol. The extracted DNA was stored at − 80°C.

Metagenome library construction and sequencing DNA samples were

quantified by Quant-iT PicoGreen dsDNA Assay (Life Technologies) and normalized to a concentration of 50 pg/mL. Illumina sequencing libraries were prepared from 100–250 pg DNA using the Nextera XT DNA Library Preparation kit (Illumina) according to the manufacturer's recommended protocol, with reaction volumes scaled accordingly. Metagenomic libraries were sequenced on the Illumina HiSeq 2500 platform, targeting 2.5 Gb of sequence per sample with 101 bp paired end reads.

Taxonomic microbiome profiling Quality control of metagenomic sequencing reads involved removal of adaptor sequences using Trim Galore! v0.4.4 followed by trimming and/or removal of low-quality reads and human sequences with KneadData v0.7.2. Samples with at least 5 million sequencing reads after quality control were included in the analysis. Species-level taxonomic profiles were generated by MetaPhlAn2 v2.9.21 (Aug 2019) using the species-specific marker database v2.94 (Jan 2019).

2.8. Statistical analyses

2.8.1. Data preprocessing for data analyses

Prior to the statistical analyses data were first log transformed and then scaled to zero mean and unit variance. Linear model with covariate adjustments was done using limma method in MetaboAnalyst 6.0. (Pang et al., 2024) Missing values and values > LOD were imputed by replacing them with half-minimum values.

2.8.2. Correlation analysis, adjusted linear models and partial correlation

Adjusted linear models linear models (limma) was applied to perform significance testing with covariate adjustments using Metaboanalyst 6.0 (Pang et al., 2024). Before selection of con-founding parameters for the adjustment, the potential association of individual parameters (maternal age, maternal BMI, maternal dietary factors related to PCBs, gestational age, weight and length of the infant, infant sex, breastfeeding status, type of formula) were investigated using Spearman correlations and then further investigating with adjusted linear models whether adjustment had an impact on the metabolome.

2.8.3. Mixture effect analysis using principal component analysis

To address multicollinearity among the 32 highly correlated exposure biomarkers (PCBs and PFAS), we performed principal component analysis (PCA) as a data-reduction approach. PCA was conducted on standardized (z-scored) exposure concentrations, using only samples with complete data across all exposure variables using R package 4.3.2 (Team, 2017). The analysis was implemented in R (version 4.3.2.) using the prcomp() function. The optimal number of components to retain was determined using parallel analysis, which compares the observed eigenvalues to those generated from randomly permuted data. Parallel analysis indicated that three principal components should be retained, together explaining the majority of variance in the exposure matrix. For interpretation, we examined the loading matrix, where loadings represent the contribution of each exposure biomarker to a given component. Loadings were visualized using bar plots, allowing identification of the compounds most strongly associated with each principal component. Component scores for the retained PCs were extracted and exported for use in subsequent statistical analyses (e.g., linear models relating exposure profiles to metabolomic outcomes).

2.8.4. Pathway analyses

Pathway analyses were done by Functional analysis module in MetaboAnalyst 6.0. The Functional analysis module approach supports functional analysis of untargeted metabolomics data generated from HRMS. The pathway analysis was done with the data of the polar and semipolar metabolites, as the pathway analysis for lipidomics data is not sufficiently robust due to the lack of exact structures of the lipids (fatty acid composition, including the position of the double bonds, cis/trans configuration). The input data for the pathway analysis comprised complete LC-HRMS data, *i.e.*, both identified and unknown metabolites, obtained in negative ionization mode. First, we performed statistical analyses using *t*-test between control and each exposure concentration, resulting in fold change, p-values and FDR values. The whole input peak list, with peak names given as their numeric mass (m/z) values for putative annotation was used for the pathway analysis. The mass tolerance for the pathway analysis was set at 7 ppm, and we also used the advanced option to select representative adducts by removing isotopic adducts as these have been already removed in the data preprocessing step. We applied both Mummichog and Gene set enrichment algorithms with p-value cutoff of 0.05 and utilized three pathway libraries: KEGG, MFN and Biosyc. In the evaluation of the results, we included only pathways showing minimum three significant compound hits, and with either of the algorithms giving a significant pathway match.

2.8.5. Microbiome analysis

To identify child microbial species whose stool abundances varied across levels of maternal PCBs exposure, mothers were classified into two exposure groups based on total PCBs levels: high exposure (above the median) and low exposure (below the median). Total PFAS exposure was defined as the sum of individual PCBs concentrations. Differences in microbial relative abundances between the high- and low-exposure groups were assessed using linear models. Covariates, including child sex, breastfeeding status, and mode of delivery, were adjusted for using the MaAsLin2 package in R (microbial abundance ~ exposure group (high vs. low) + sex + breastfeeding status + mode of delivery). Spearman correlation coefficients were computed using the cor function in R, and results were visualized using the ggplot2 and pheatmap packages.

3. Results

3.1. Participant characteristics

Participant characteristics and distribution of persistent organic pollutants in the mothers (n = 68) from the EDIA cohort are presented in Table 1. The median age of the mother was 32.6 years. The majority of the offsprings were born via vaginal delivery (88.5%) at a mean gestational age of 39.7 weeks. The median weight of the offsprings was 3500 g and the sex distribution was balanced (35/38 male/female infants). In this cohort, 53% of the infants were fully breastfed at the age of 3 months, 6% were not breastfed at all, and 37% were fully breastfed for less than 2 weeks. The proportion of infants who received any breast milk varied from 91.5% at the age of 3 months to 47.1% at 12 months (Koivusaari et al., 2023).

The detection rates of POPs varied between 8 and 100% depending on the compound. For PCBs, PCB153 and PCB180 were the most abundant compounds while PCB206 and PCB209 were detected at low concentrations. Among the studied OC pesticides, p,p'-DDE and HCB were detected in more than 80% of the study participants while cis- and *trans*-chlordane were only detected in 8% and 9% of the subjects, respectively. The two most abundant PFAS detected were PFOS and PFOA, detected in all subjects. PCBs and PFAS showed clear correlation with each other, probably due to similar dietary sources of exposure. When compared to other mother–child cohort studies, we found that concentrations of POPs in maternal serum in our study are comparable to those previously reported in Europe (Haug et al., 2009; Haug et al., 2011; Haug et al., 2018; Tamayo-Uria et al., 2019).

3.2. Impact of exposure on clinical parameters

Fig. 1 illustrates associations between prenatal exposure and maternal age, BMI, and infant related parameters at birth and at three months of age. Maternal age was positively associated with several PCBs, while there was no significant association between the maternal age and PFAS. Some PFAS showed positive association with maternal BMI, while there were no significant associations between PCBs and

Table 1
Characteristics of the study population.

Parameter	Median (range)	
Mother-infant dyads (n)	73	
Maternal delivery age (years)	32.6 (20.9–45.8)	
Way of delivery	88.5% vaginal, 11.5% Cesarian section	
Gestational age (weeks)	39.7 (36.4–42.3)	
Sex of the baby (male/female)	35/38	
Child weight (g)		
0 months (birth)	3500 (2600–4720)	
3 months	6200 (4300–8200)	
Child length (cm)		
0 months (birth)	50.1 (46.0–55.0)	
3 months	62.2 (51.5–67.5)	
Maternal POPs	**Median (min–max) pg/ml**	**Detection frequency**
PCB74	13.1 (2.73–44.19)	87%
PCB99	19.23 (8.8–72.09)	68%
PCB118	38.18 (19.2–137.21)	54%
PCB105	12.94 (6.92–41.86)	44%
PCB153	117.6 (51.2–467.44)	99%
PCB138	87.06 (34.4–383.72)	99%
PCB156	8.33 (1.67–32.56)	98%
PCB157	1.43 (ns-6.98)	89%
PCB180	59.09 (16–223.26)	100%
PCB170	25.45 (4.44–90.0)	100%
PCB189	0 (nd-3.45)	49%
PCB194	6.09 (nd-27.91)	98%
PCB206	0.74 (md-2.11)	51%
PCB209	0.82 (nd-4.0)	54%
HCB	143.33 (75.86–451.16)	92%
trans-Nonachlordane	7.41 (nd-41.0)	71%
cis-chlordane	3.06 (nd-54.7)	9%
Trans-chlordane		8%
p,p-DDE		100%
Maternal PFAS	**Median (min–max) ng/ml**	
PFBA	0.15 (nd-1.41)	17%
PFPeA	0.11 (nd-0.92)	12%
PFHpA	0.04 (nd-3.02)	21%
PFHxS	0.32 (0.08–1.24)	100%
PFOA	0.99 (0.28–3.6)	100%
PFHpS	0.04 (nd-0.18)	34%
PFNA	1.43 (0.05–0.52)	70%
PFOS	1.32 (0.04–13.32)	100%
PFDA	0.18 (0.05–0.52)	75%
PFUnDA	0.20 (nd-0.54)	94%

maternal BMI. Length of any breastfeeding was positively associated with maternal levels of *cis*-chlordane, PCB99, PCB157, PCB209 and PFPeA and inversely with PFOS. Gestational age, infant sex or birth weight did not show any associations with PCBs or PFAS while birth length was inversely associated with PCB19 and PCB209. The latter showed an inverse association with the infant length also at 3 months of age. Fecal Beta2 defensin at 3 months of age was positively associated with PCB206 and fecal calprotectin at three months of age was positively associated with PFOS. The exposure profiles were also showing significant positive correlation with each other (Supplementary Fig. 1) with also significant positive correlation within PCBs and PFAS.

The maternal dietary data was analysed to assess the dietary sources of POPs. For PFAS, shellfish showed the strongest correlation with PFAS and also fish, cereals and fruit juice were correlating with PFAS levels. Dietary item-specific analyses revealed that dietary items such as fish, shellfish, leaf vegetables, mushroom, and nuts and seeds were positively correlated with several PCBs and OC pesticides whereas poultry, lamb, oats and bar, coffee, pasta, and soft drink, consumption tended to be inversely associated with PCBs and OC pesticides. We further assessed whether POP-related dietary items were associated with the infant metabolome. Although several metabolites showed nominal associations, only one (between maternal fish intake and isopentanoic acid) remained significant after FDR correction.

Based on the results, we further selected maternal age, maternal BMI and breastfeeding as covariates for adjustment of the data analyses. Because maternal POP levels also determine exposure through breast milk, early postnatal transfer of POPs may overlap with prenatal exposure. Although our models were adjusted for breastfeeding duration, some residual confounding by lactational exposure may remain, and the observed associations should therefore be interpreted as reflecting combined prenatal and early postnatal exposure.

3.3. Impact of delivery type and exclusive breastfeeding on metabolome

Given that birth method and breastfeeding are major early-life factors shaping both microbiota composition and metabolic profiles, and PFAS exposure has previously been linked to breastfeeding duration (Hoadley et al., 2023), we initially assessed their associations in our cohort to account for their potential confounding influence when interpreting POP-related effects. Majority of the children in this study were born by vaginal delivery, and only 11.5% by caesarean section. The mode of delivery was associated at nominal level with multiple metabolites that are known to be linked with gut microbiota, particularly with secondary bile acids, with these compounds showing lower level in children born with caesarean section. However, of the identified metabolites, only glycohyocholic acid remained significant after FDR correction (FC = −1.63, p = 9.3*10–5). Functional pathway analysis using the whole nontarget data showed that several metabolic pathways were affected by the mode of delivery, particularly those related to bile acid and amino acid metabolism (Table 3).

In this cohort, 53% of the infants were fully breastfed at the age of three months, 6% were not breastfed at all, and 37% were fully breastfed for less than two weeks. When comparing the metabolic profiles of those children that were fully breastfed for the first three months, with those that were either fully breastfed for less than two weeks or less than three months, significant differences could be observed (Supplementary Table 1). As reported earlier, there was also difference in the metabolic profiles in those children that were not breastfed but were fed with different types of formulas (Lamichhane et al., 2022).

3.4. Association of the metabolome with prenatal POP exposure

Prenatal PCB exposure had a major impact on metabolic profiles of the infants, especially on lipids (Fig. 2, Supplementary Table 2). Particularly, the concentrations of PCB153, PCB138, PCB156, PCB180, PCB170 and PCB194 showed significant positive association with large number of lipids, particularly with acylcarnitines, cholesterol esters, ceramides, PCs and SMs. PCBs also showed some inverse associations with amino acids (AA) bile acids (BA) and positive associations with free fatty acids (FFA) and their derivatives. Four PCBs (PCB99, PCB118, PCB105 and PCB138) were positively associated with the SCFA acetic acid while three PCBs (PCB156, PCB180 and PCB17) showed an inverse association with SCFA butyric acid. HCB was also positively associated with one of the SCFAs (valeric acid). PCBs showed also associations with diet and gut derived compounds, such as phytanic acid and syringic acid.

Prenatal exposure to PFAS was associated with changes both in lipids and other metabolites (Fig. 3, Supplementary Table 3). Particularly, PFHxS, PFOA, PFNA, PFOS, PFDA and PFUnDA showed significant associations with lipids. Acylcarnitines and ceramides and phospholipids containing polyunsaturated fatty acyls, including alkylether lipids were positively associated with several PFAS, with PFUnDA in particular. Also several SMs showed positive associations with PFAS. Amino acids showed mainly negative associations with PFAS, except for taurine,

Table 2
LC-MS conditions for the methods utilised in metabolomics analysis.

Conditions	Polar/semipolar compounds	Lipidomics	SCFA and other polar metabolites
Injection volume	10 μL	1 μL	5 μL
Column	C18 precolumn (Waters Corporation, Wexford, Ireland) and an inline filter, pore size 0.2 μm (Waters Corporation). + ACQUITY UPLC BEH C18 column (2.1 mm × 100 mm, particle size 1.7 μm) by Waters (Milford, MA, USA)	C18 precolumn (Waters Corporation) and an inline filter, pore size 0,2 μm (Waters Corporation). + ACQUITY UPLC BEH C18 column (2.1 mm × 100 mm, particle size 1.7 μm) by Waters	Acquity UPLC BEH C18 column (2.1 x 100 mm, 1.7 μm; Waters)
Mobile phases	A: H_2O:MeOH (v/v 70:30) with 2 mM ammonium acetate B: MeOH with containing 2 mM ammonium acetate	A: 10 mM ammonium acetate and 0.1% Formic Acid in H_2OB: Acetonitrile:Isopropanol (v/v 1:1) with 0.1% Formic Acid and 10 mM ammonium acetate	A: 0.1 % (v/v) formic acid in H_2O B: acetonitrile
Gradient	• 0–1.5 min: B was increased from 5% to 30% • 1.5–4.5 min: B increased to 70%; • 4.5–7.5 min: B increased to 100% and held for 5.5 min. • A re-equilibration with 30% B 6 min	• 0–2 min: B was increased from 35% to 80% • 2–7 min: B increased to 100% • 7–14 min: B was held at 100%. • A re-equilibration with 5% B 7 min	• 0 – 2 min: 90% A and 10% B • 2–6 min: increase to 90% B • 6–10 min 90% B • re-equilibration with 10% B for 3 min
Flow rate	0.4 mL/min	0.4 mL/min	0.4 mL/min
MS conditions	Dual ESI ionization source with capillary voltage 4.5 kV, nozzle voltage 1500 V, N_2 pressure in the nebulizer was 21 psi and the N_2 flow rate and temperature as sheath gas was 11 L/min and 379 °C, respectively. Drying gas flow was set to 10 L/min and temperature to 150 °C. *m/z* range 50–1700 in negative ion mode.	Dual ESI ionization source with capillary voltage 3.64 kV, nozzle voltage 1500 V, N_2 pressure in the nebulizer was 21 psi and the N2 flow rate and temperature as sheath gas was 11 L/min and 379 °C, respectively. Drying gas flow was set to 10 L/min and temperature to 193 °C. *m/z* range 100–1700 in positive ion mode	Dual ESI source with capillary voltage 3.6 kV, nozzle voltage 1500 V, and N_2 pressure at nebulizer, flow rate and temperature as sheath gas set at 21 psi, 10 L/min and 379 °C, respectively. Drying gas flow was set to 10 L/min and temperature to 150 °C. *m/z* range 50–1700 in negative ion mode

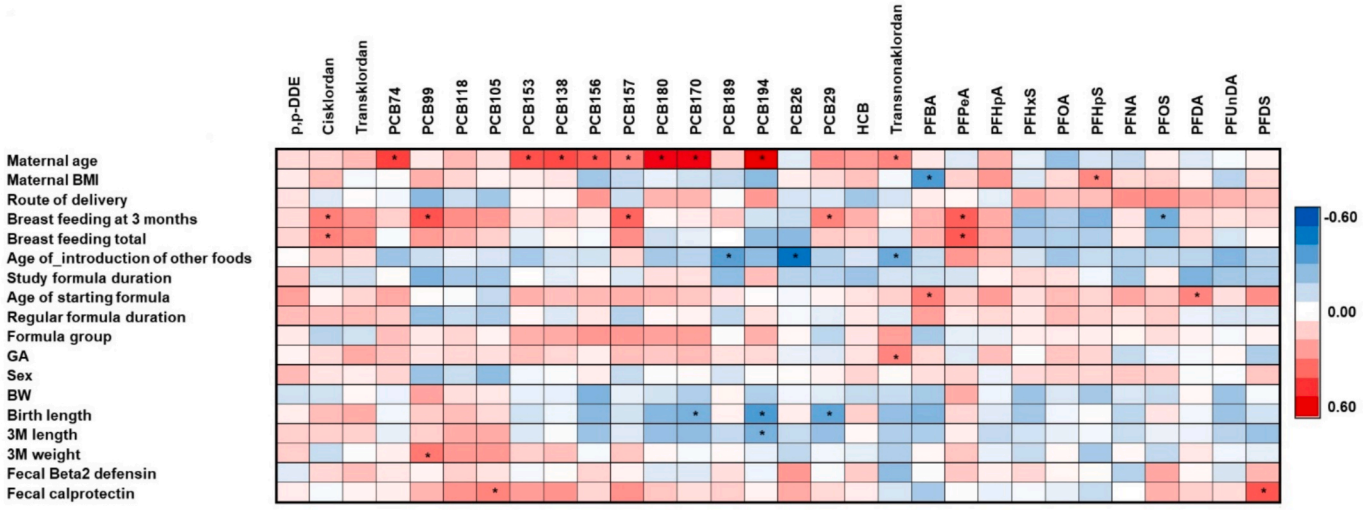

Fig. 1. Spearman correlation between clinical parameters and maternal PCBs and PFAS. Red: positive association, blue: negative association, with strength of the colour indicating the strength of the correlation and significant correlations marked as *.

Table 3
Pathway analysis of the impact of delivery way.

Library	Pathway	Total_Size	Hits	Sig_Hits	Mummichog_Pvals	GSEA_Pvals	Combined_Pvals
KEGG	(S)-reticuline biosynthesis II	16	8	3	0.568	**0.043**	0.1160
KEGG	4-hydroxybenzoate biosynthesis	18	7	4	0.195	**0.043**	0.0489
KEGG	4-hydroxy-phenylpyruvate biosynthesis	4	4	3	0.124	**0.026**	0.0216
MFN	Bile acid biosynthesis	82	53	32	**0.000**	0.999	0.0000
KEGG, Biosyc	bile acid biosynthesis, neutral pathway	48	18	11	**0.019**	0.999	0.0929
MFN	Biopterin metabolism	22	3	3	**0.027**	**0.037**	0.0078
KEGG	Catecholamine biosynthesis	15	5	5	**0.005**	0.235	0.0090
MFN	Linoleate metabolism	46	26	15	**0.003**	0.999	0.0182
MFN	N-Glycan Degradation	16	3	3	**0.027**	0.407	0.0598
MFN	Omega-3 fatty acid metabolism	39	4	4	**0.008**	0.999	0.0461
Biosyc, KEGG	phenylalanine degradation I (aerobic)	10	3	3	**0.003**	**0.029**	0.0010
KEGG	tRNA charging	64	19	11	**0.031**	0.999	0.1382
KEGG	tryptophan degradation to 2-amino-3-carboxy-muconate semialdehyde	13	5	4	0.052	**0.048**	0.0174
Biosyc, KEGG	tyrosine biosynthesis IV	5	3	3	**0.003**	**0.029**	0.0010
Biosyc, KEGG	tyrosine degradation I	13	6	3	**0.045**	**0.035**	0.0118

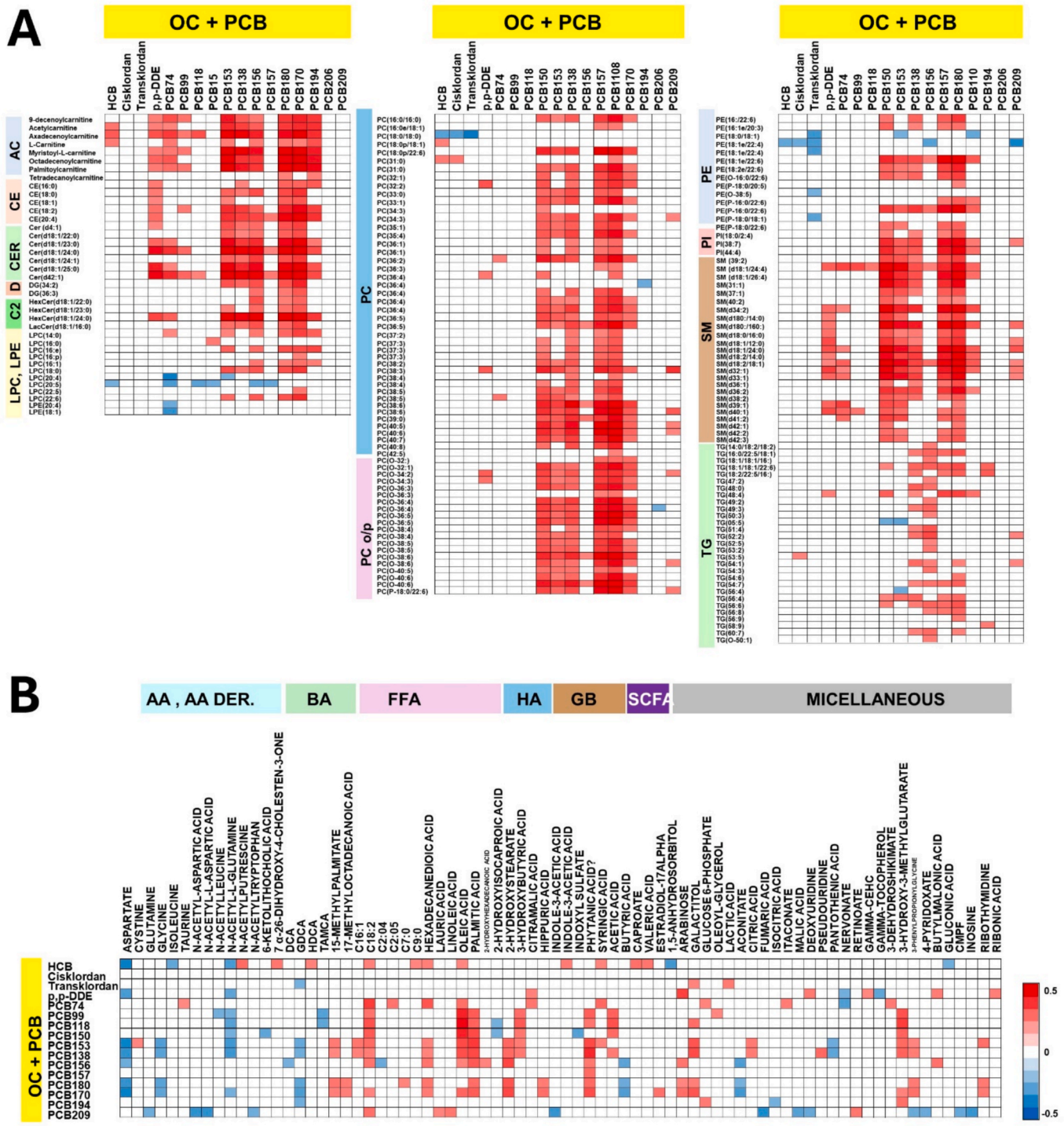

Fig. 2. Adjusted Spearman correlations (adjusted with maternal age, BMI, length of breastfeeding at 3 months) between OC and PCBs and A) lipids and B) with polar and semipolar metabolites. Only significant associations given. Red: positive association, blue: negative association. Abbreviations: AA- amino acids, AC- acylcarnitines, BA- bile acids, CE- cholesterol esters, Cer_ceramides, C2 – hexylceramides, D_- diacylglycerols, FFA- free fatty acids, HA – hydroxy acids, GB – gut microbiota derived metabolites, LPC- lysophosphatidylcholines, LPE- lysophosphatidylethanolamines, PC- phosphatidylcholines, PCo/p alkylether PCs, PE – phosphatidylethanolamines, PE o/p alkylether Pes, PI – phosphatidylinositols, SCFA – short-chain fatty acids, SM- sphingomyelins, TG – triacylglycerols.

tryptophan and tyrosine that were positively associated with PFHxS, PFHpA and PFPeA. Most bile acids were inversely associated with PFAS, except for CDCA which showed a positive association with PFHpA and HDCA. Several gut microbiota-derived metabolites (Indole-3-acetic acid, hippuric acid, indoxyl sulfate) were positively associated with PFAS. Oxobutanoic acid and valeric acid were positively associated with PFUnDA, Several PFAS showed positive associations with sugar derivatives arabinose, ertyhtonic acid and ribonic acid, vitamin E derivative gamma-CEHC and nucleosides ribothymidine and deoxyuridine.

Principal component analysis of the 32 PCB and PFAS exposure biomarkers revealed strong correlations among multiple compounds. Horn's parallel analysis supported the retention of three principal components, which together explained a substantial proportion of the

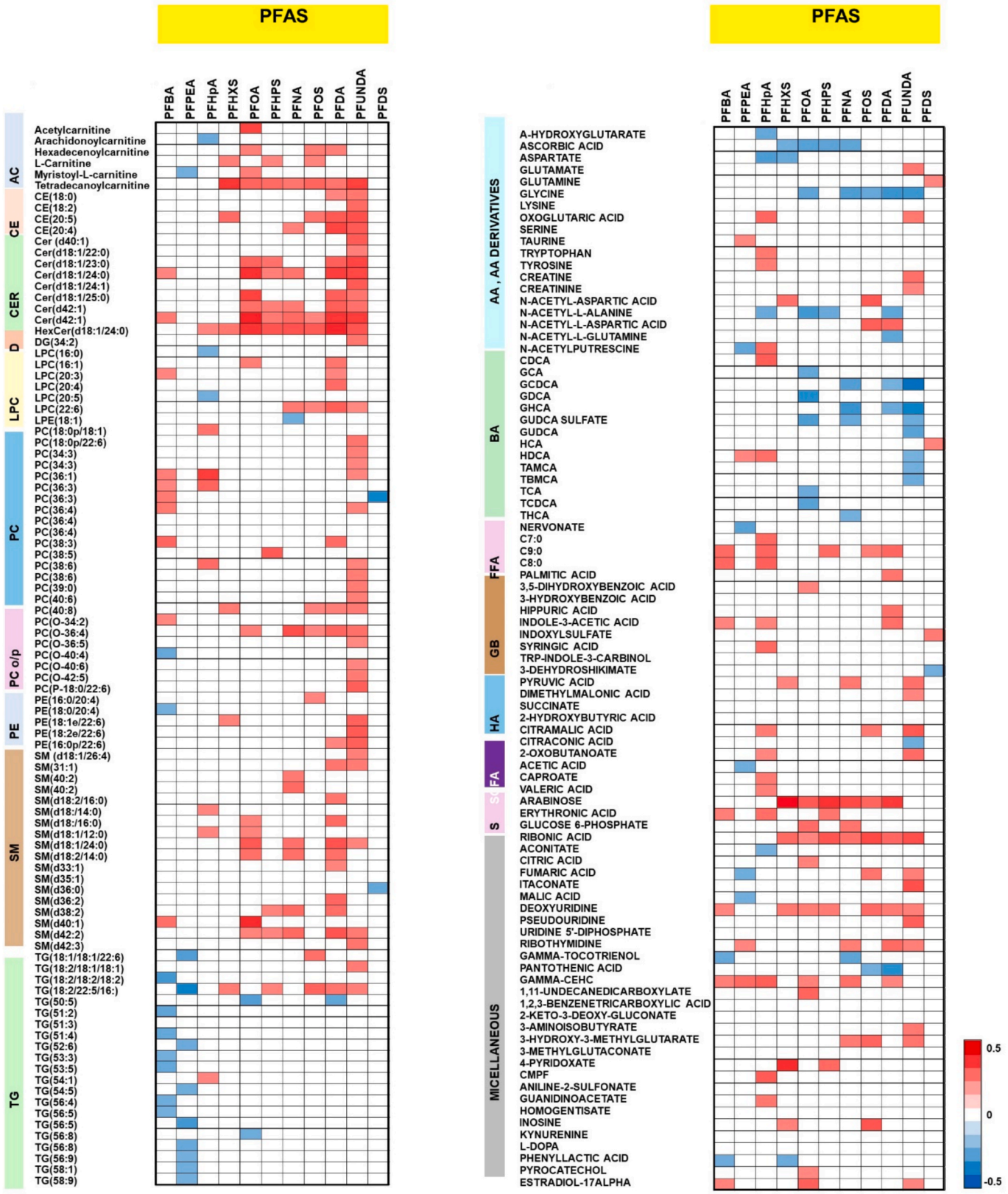

Fig. 3. Adjusted Spearman correlations (maternal age, BMI, length of breastfeeding at 3 months) between PFAS and A) lipids and B) with polar and semipolar metabolites. Only significant associations given. Red: positive association, blue: negative association. Abbreviations: AA- amino acids, AC- acylcarnitines, BA- bile acids, CE- cholesterol esters, Cer_ceramides, C2 – hexylceramides, D_- diacylglycerols, FFA- free fatty acids, HA – hydroxy acids, GB – gut microbiota derived metabolites, LPC- lysophosphatidylcholines, LPE- lysophosphatidylethanolamines, PC- phosphatidylcholines, PCo/p alkylether PCs, PE – phosphatidylethanolamines, PE o/p alkylether Pes, PI – phosphatidylinositols, SCFA – short-chain fatty acids, SM- sphingomyelins, TG – triacylglycerols.

total variance (Supplementary Fig. 2). Examination of the loading matrix indicated that each component reflected distinct co-exposure patterns. PC1 showed relatively high positive loadings for several PCB congeners, particularly PCB180, PCB170, PCB194, PCB153, PCB156, PCB138, PCB157, PCB74, and PCB118.

PC2 was characterized by high positive loadings for PFOS, PFHxS, PFOA, PFNA, and PFDA, and negative loadings for PCB99, PCB118, PCB105, and HCB.

PC3 exhibited negative loadings for PFNA, PFDA, transchlordan, and cischlordan, and positive loadings for PCB180, PCB170, and PCB194. Individual PC scores were then calculated for all participants and used in adjusted linear models to assess associations with the infant metabolome (Supplementary Table 4). At the nominal p-value level, a large number of polar metabolites and lipids were associated with the three PCs. After FDR correction, PC1 remained significantly—predominantly inversely—associated with several triacylglycerols, whereas PC3 showed a positive association with a single TG species (TG(48:4)).

3.5. Pathway analysis

We then performed pathway analysis on the infant metabolome using metabolic pathway enrichment based on the mummichog and GSEA algorithms, with the full data on non-target analysis for those PCBs and PFAS showing the strongest metabolic dysregulation (Supplementary Table 5). It should be noted that while this non-target data also includes large number of lipids, the neutral lipids (CE, DG, TG) are not included in the analysis. The lipid pathway analysis tools are not currently sufficiently robust.

For PCBs, the major pathways associated with the exposure were related to fatty acid metabolism, as well as bile acid and steroid hormone metabolism, with individual PCBs showing similarities (Fig. 4A). PCB153 showed the strongest effect on metabolic pathways, while PCB180 and PCB138 had less specific impact.

PFAS showed more diverse association with metabolic pathways (Fig. 4B), with specifically multiple fatty acid and amino acid metabolism related pathways were affected, as well as bile acid metabolism. Interestingly, PFUnDA showed the highest number of dysregulated pathways while PFOA was associated particularly strongly with dysregulated bile acid metabolism.

3.6. Impact of exposure on gut microbiota

Prenatal exposure to PCBs was associated with shifts in the gut microbiome composition of infants at 3 months of age (n = 62, Fig. 5). To investigate this effect, we categorized infants into high and low exposure groups based on total maternal PCB levels and compared their gut microbiome profiles (Fig. 5A). We identified 11 microbial species that significantly differed between the two groups (Supplementary Table 6). Species including *Bifidobacterium bifidum*, *Prevotella timonensis*, *Actinomyces neuii*, *Lactobacillus paragasseri*, *Dolosigranulum pigrum*, and *Streptococcus oralis* were reduced in the high exposure group while, *Erysipelatoclostridium ramosum*, *Adlercreutzia equolifaciens*, *Denitrobacterium detoxificans*, *Asaccharobacter celatus*, and *Veillonella rodentium* were more abundant. We next sought to determine the associations between individual PCBs and the differentially abundant microbial species between high and low exposure group. Using Spearman rank correlation, we assessed relationships between 19 measured PCBs and the identified microbial taxa. *Cis*- and *trans*-chlordane showed positive correlations with several bacteria reduced in the high exposure group, including the probiotics *B. bifidum* and *L. paragasseri*. On the other hand, multiple PCBs (PCB-74, PCB-99, PCB-105, PCB-118, PCB138, PCB153, PCB156, PCB157, PCB170, PCB180, PCB189, PCB194, PCB206) were inversely associated with these species (Fig. 5b).

Similarly, we examined associations between the circulatory metabolome and the microbial taxa that were differentially abundant between the high and low PCB exposure groups in 3-month-old infant samples. Microbes that were reduced in the high exposure group including *Bifidobacterium bifidum*, *Prevotella timonensis*, *Actinomyces neuii*, *Lactobacillus paragasseri*, *Dolosigranulum pigrum*, and *Streptococcus oralis* showed a consistent pattern of inverseassociations with amino acids, amino acid derivatives, and fatty acids, including short-chain fatty acids (SCFAs) and long-chain fatty acids (LCFAs) and microbial tryptophan metabolite Indole-3-acetic acid (Fig. 6A). These same taxa also showed inverse associations with sphingolipids (SM, and Cer) and glycerophospholipids (PC and LPC), with the exception of *Bifidobacterium*, which did not reflect this trend (Fig. 6B). In contrast, microbial species enriched in the high exposure group such as Erysipelatoclostridium *ramosum*, *Adlercreutzia equolifaciens*, *Denitrobacterium detoxificans*, *Asaccharobacter celatus*, and *Veillonella rodentium* were strongly positively associated with secondary bile acid (HDCA) and triglyceride levels. *Denitrobacterium detoxificans*, a strictly anaerobic bacterium more commonly described in environmental or ruminant-associated ecosystems, was detected at low abundance in infant stool samples. Given the dynamic nature of the infant gut microbiota and the limitations of species-level taxonomic resolution in 16S rRNA sequencing, this finding likely reflects transient colonization or assignment to a closely related anaerobic taxon rather than stable presence of this species.

4. Discussion

In the current study, we observed significant associations between prenatal exposure to persistent organic pollutants (POPs) and the metabolic profiles and gut microbiota composition in infants at three months of age. However, because maternal POP body burden also determines infant exposure during early lactation, postnatal exposure through breastfeeding likely overlaps with prenatal exposure. Although all analyses were adjusted for breastfeeding duration to account for this contribution, residual confounding by early postnatal exposure cannot be fully excluded. Therefore, the observed associations likely reflect a combination of prenatal and early postnatal exposure. Notably, pathway analysis revealed distinct metabolic impacts between PFAS and PCBs, with PCBs showing more pronounced and consistent associations. Although strong associations were observed between POP exposure and lipids, including neutral lipid classes such as cholesterol esters and triacylglycerols, these lipids were not included in the pathway analysis due to current limitations in lipid pathway annotation, and this exclusion should be considered a limitation when interpreting pathway-level findings.

Previous work in this cohort has examined PFAS-related effects on cord-blood metabolism and on microbiota-related outcomes at three months of age, but either the metabolic profiling at this early postnatal time point nor the association between PCB exposure on both metabolome and microbiota has not been assessed previously. Our findings therefore provide novel insight into PCB-associated metabolic alterations in early infancy. When viewed together with prior PFAS-focused analyses, the present results highlight both shared and distinct exposure–metabolome relationships for different classes of persistent organic pollutants.

Our findings suggest that prenatal PCB exposure is linked to disruptions in both lipid metabolism and microbial-derived metabolic pathways. The main contributors were non-planar PCBs (PCB153, PCB138, PCB180, PCB170, and PCB194), with one planar congener (PCB156) also showing significant effects. Specifically, we observed strong positive associations with PCBs and acylcarnitine, cholesterol esters, ceramides, phosphatidylcholines, and sphingomyelins. Particularly phospholipids, ceramides and acylcarnitines. These findings are consistent with previous reports identifying PCBs as metabolism-disrupting chemicals (MDCs), although detailed lipid class-specific effects remain underexplored. In support of our findings, a previous human study reported a positive association between PCB levels and serum triglycerides, even within normal exposure ranges (Aminian et al., 2020). Similarly, experimental studies in pigs exposed to high

levels of PCBs have shown alterations in fatty acid metabolism, glycerophospholipid pathways, and the tryptophan–kynurenine axis (Hernández-Mesa et al., 2022). Disruption of lipid metabolism—particularly elevations in ceramides, acylcarnitines, and cholesterol esters—has been implicated in the development of insulin resistance, hepatic steatosis, and cardiometabolic diseases later in life (Luukkonen et al., 2016; Bazarganipour et al., 2019). Increased levels of ceramides, for instance, are associated with impaired insulin signalling, mitochondrial dysfunction, and inflammation, which are key features of metabolic syndrome (Roszczyc-Owsiejczuk 2021; Gaggini et al., 2022; Pan et al., 2024). Likewise, elevated acylcarnitines suggest impaired fatty acid oxidation, potentially leading to mitochondrial stress and lipid accumulation (Mihalik et al., 2010; McCoin et al., 2015).

The PCA patterns illustrate that several PCB congeners co-occur and exhibit shared associations with metabolic outcomes, consistent with a mixture effect rather than isolated chemical action. We also observed that PCBs were associated with changes in gut microbial metabolites, including short-chain fatty acids (SCFAs) and other microbially derived compounds such as phytanic acid and syringic acid, suggesting a broader impact on host–microbiome metabolic interactions. In contrast, the metabolic effects of PFAS were more modest and less consistent. However, PFAS exposure was still associated with increases in ceramides, cholesterol esters, and acylcarnitines. Interestingly, shorter-chain PFAS (PFBA and PFPeA) showed negative associations with triglycerides—a pattern not observed for longer-chain PFAS. Several bile acids were negatively associated with PFAS, aligning with previous studies (Sinisalu et al., 2020; Hyötyläinen et al., 2024). At the pathway level, PCB exposure was linked to alterations in fatty acid, bile acid, and steroid hormone metabolism. PFAS exposure, while partially overlapping in its impact, also showed broader dysregulation of amino acid metabolic pathways. The observed reduction in bile acids may affect lipid digestion and nutrient absorption and impair gut-liver signaling,

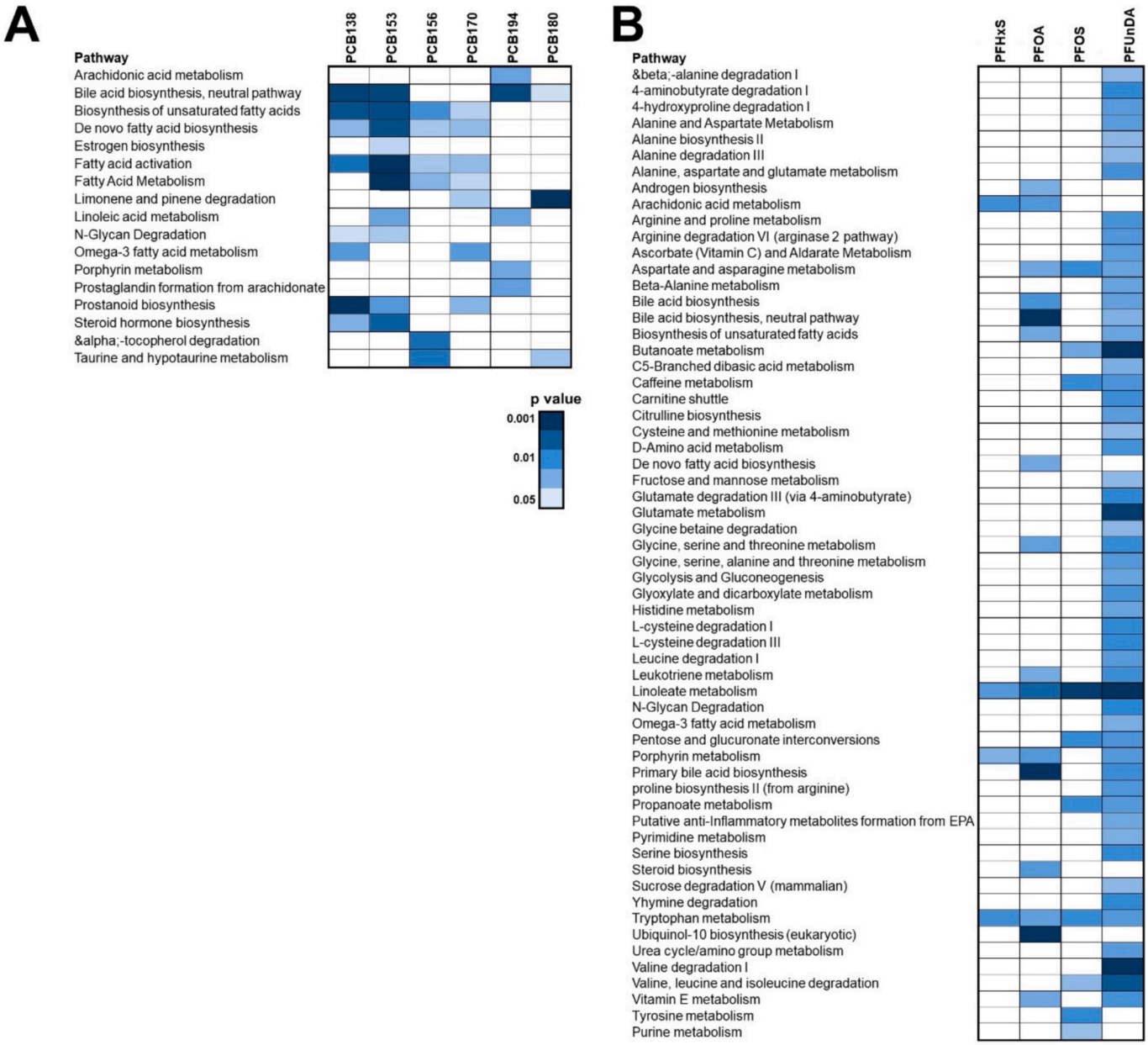

Fig. 4. Heatmap of dysregulated metabolic pathways associated with A) PCB and B) PFAS exposures. *p* values are indicated using a blue colour scale ranging from $p < 0.001$ (dark blue) to $p = 0.05$ (light blue), with white indicating no significant association. For each pathway, the minimum *p* value derived from either the mummichog or GSEA algorithm is shown. See Supplementary Table 5 for detailed results.

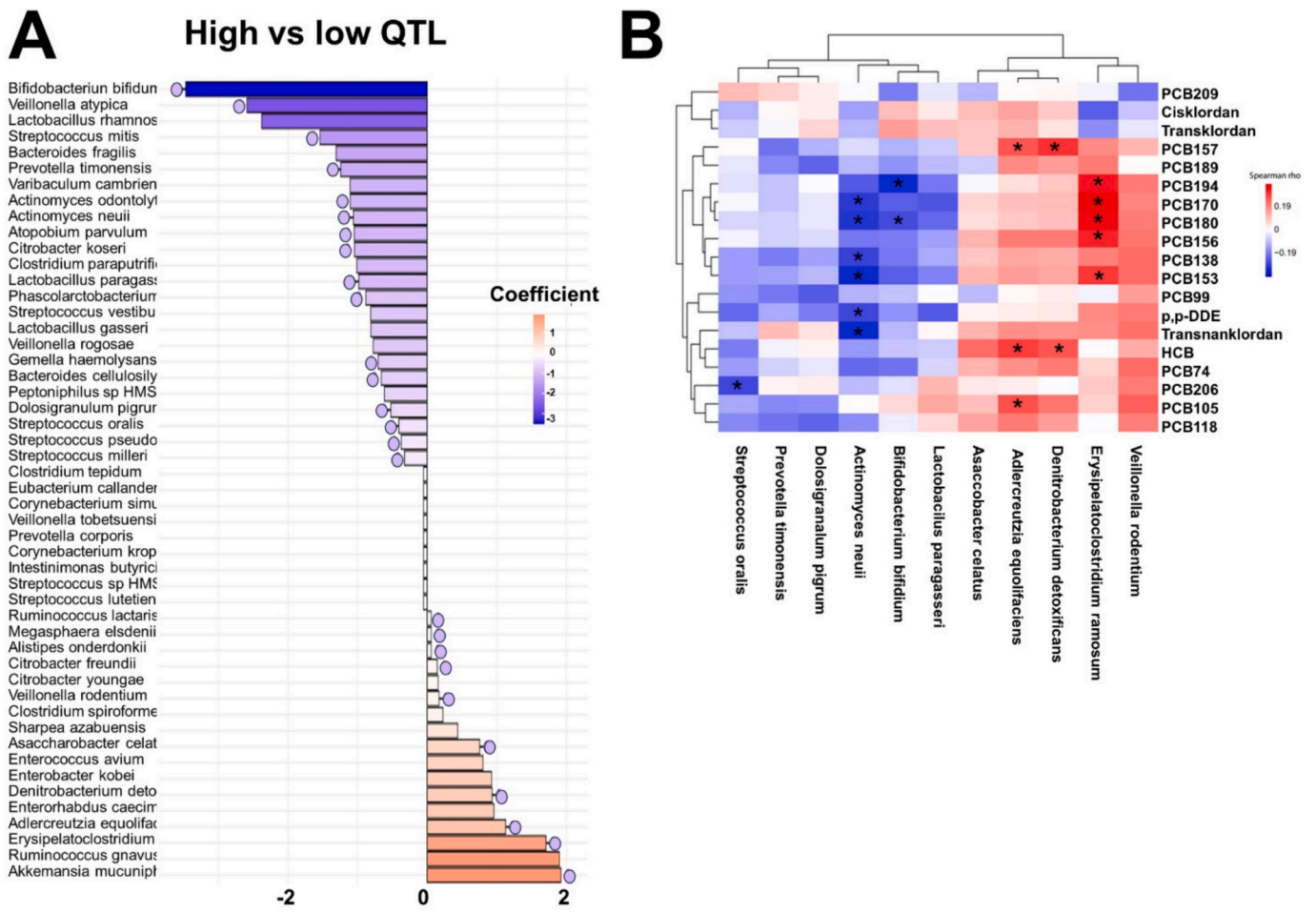

Fig. 5. Effects of maternal PCB exposure on the infant gut microbiome. A) Bar plots showing the correlation coefficients for the association between relative abundances of gut microbiota in 3-month-old infants across high and low PCB exposure groups. Red bars represent positive correlations, while blue bars represent negative correlations, as determined by linear regression models. The bars feature a thin line (stick) topped with a pink circle (lollipop head), representing a nominal p value < 0.05. Adjusted p values (corrected for multiple comparisons using the Benjamini-Hochberg method) are available in Supplementary Table 6. B) Correlations between maternal PCB levels and microbial species in infants. Spearman rho were performed between individual PCBsand microbial taxa that differed between high exposure (above the median) and low exposure (below the median) groups. The colour scale represents the correlation strength (blue = negative, red = positive). An asterisk (*) indicates correlations with a nominal p-value < 0.05.; adjusted p values (corrected for multiple comparisons using the Benjamini-Hochberg method) are available in Supplementary Table 7.

contributing to dyslipidemia and altered energy homeostasis.

Our findings suggest that PCBs may modulate host metabolism also indirectly through alterations in the gut microbiota. Several microbial taxa associated with PCB exposure have previously been linked to metabolic health. For example, a reduced abundance of *Bifidobacterium bifidum*observed in our high exposure group has been associated with increased visceral adiposity, BMI, serum triglycerides, and fatty liver in adults. Supplementation with *B. bifidum* has been shown to enhance bile acid signaling and support oxidative phosphorylation in adipose tissue, highlighting its role in metabolic homeostasis (Kim et al., 2022). *Erysipelatoclostridium ramosum,* which was enriched in infants with higher PCB exposure, has been shown to promote diet-induced obesity in mice by upregulating intestinal nutrient transporters, thereby enhancing glucose and fatty acid absorption (Woting et al., 2014). It is also regulated by maternal milk-derived secretory IgA (SIgA), plays a key role in immune development, and has been identified in *meta*-analyses as a keystone taxon associated with allergy risk in infancy (Donald et al., 2025; Peng et al., 2024). *Prevotella timonensis,* another species linked to PCB exposure in our study, has been associated with increased proinflammatory cytokines such as TNF-α and IL-1β (Wang et al., 2022), suggesting a potential role in low-grade inflammation. Conversely, *Lactobacillus paragasseri*, which was depleted in the high exposure group, has demonstrated beneficial effects in animal models, including attenuation of insulin resistance and fatty liver via suppression of oxidative stress and inflammation (Kim et al. 2025) Similarly, related strains such as *Lactobacillus paracasei*, isolated from human milk, have been shown to ameliorate hyperlipidemia by modulating the gut microbiota, enhancing hepatic lipid and bile acid metabolism, and increasing cholesterol efflux (Yao et al., 2025).

In addition, some taxa linked to PCB exposure may also be involved in host metabolic signaling through bioactive metabolite production. For instance, *Adlercreutzia equolifaciens* has been identified as a beneficial microbe involved in the metabolism of isoflavones and production of short-chain fatty acids and amino acid derivatives, with potential anti-inflammatory and metabolic regulatory effects (Wu et al., 2024; Kumar et al., 2025). *Asaccharobacter celatus*, another isoflavone-metabolizing bacterium, may similarly contribute to host metabolic homeostasis through its capacity to transform dietary polyphenols (Takagaki and Nanjo 2016).

Interestingly, we observed that metabolites positively associated with PCB exposure were inversely correlated with several microbial taxa that were depleted in the high exposure group. This pattern suggests a potential mediating role of the gut microbiota, whereby PCB-induced alterations in microbial composition may disrupt host–microbe

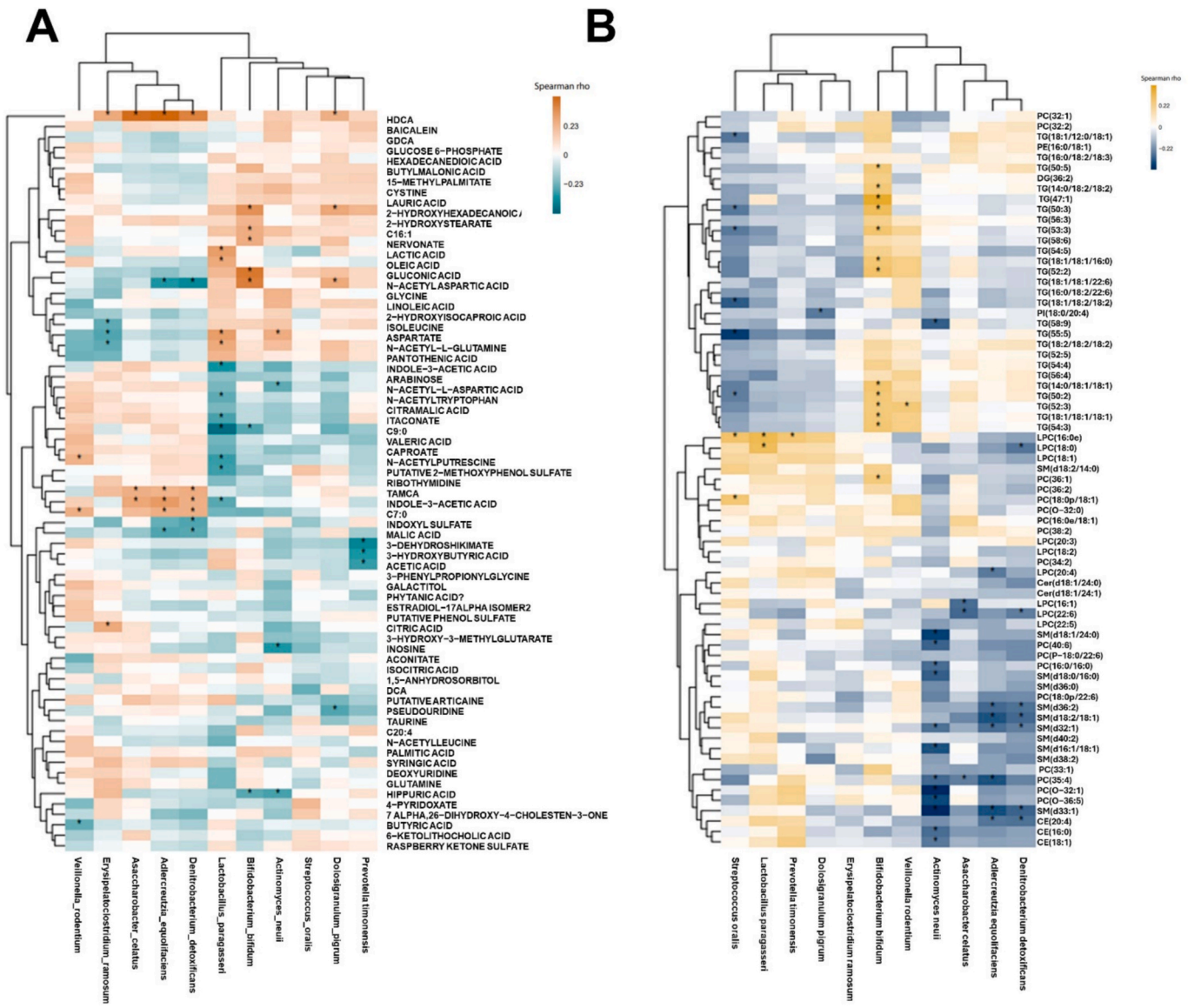

Fig. 6. Association between microbial features and the circulatory metabolome. Each cell represents the Spearman correlation coefficient between A) polar metabolites and B) lipids (rows) and microbial features (columns). Colours indicate the direction and magnitude of correlation: for A) green tones represent negative correlations, white indicates near-zero correlations, and orange-red tones indicate positive correlations; for B) blue tones represent negative correlations, white indicates near-zero correlations, and gold tones indicate positive correlations. An asterisk (*) denotes correlations with a nominal p-value < 0.05. Adjusted p-values (corrected for multiple comparisons using the Benjamini-Hochberg method) are provided in Supplementary Tables 8 and 9.

metabolic interactions, contributing to the accumulation of specific lipid and amino acid metabolites. Such triangular relationships highlight the complex interplay between environmental exposures, the gut microbiome, and systemic metabolism, and support the hypothesis that the microbiota may buffer or amplify the metabolic impacts of environmental toxicants. Our results align with emerging evidence from animal studies indicating that PCB exposure disrupts gut microbial composition, with implications for host lipid and bile acid metabolism (Cheng et al., 2018; Lim et al., 2020; Dean et al., 2025). For example, studies in rodents have shown that gut microbiota modulate PCB-induced effects on bile acid homeostasis and hepatic gene expression (Cheng et al., 2018). Previous work has also revealed that the gut microbiota influences PCB-mediated hepatic responses (Lim et al., 2020). However, human studies on PCB–microbiome interactions remain limited, and our study contributes novel data in this area.

Disruptions in host microbiota metabolic interactions during early life may have long-term consequences for health. (Lamichhane et al., 2018; Hou et al., 2022). PCBs are known to interfere with hepatic lipid metabolism, a key regulator of systemic energy balance. Alterations in bile acid signaling—central to the gut–liver axis—represent a potential mechanism linking PCB exposure to broader metabolic changes (Shi et al., 2012; Albillos et al., 2020; Guzior and Quinn 2021). Our findings support this hypothesis, as both PCBs and PFAS were inversely associated with bile acid concentrations, and pathway analysis identified bile acid and steroid metabolism as key disrupted networks. These observations are consistent with our prior work on PFAS and bile acid metabolism and suggest that PCBs may exert similar effects (Sen et al. 2022). It is likely that PCBs exert a similar impact, as previously hypothesized and further substantiated by pathways analysis suggesting that the strongest effect of exposure was on bile acid and steroid hormone metabolism pathways.

Together, our results demonstrate a strong association between prenatal PCB exposure and disruptions in lipid metabolism, gut microbial composition, and microbially derived metabolites in early infancy. Among the PCB congeners, PCB153, PCB138, and PCB180 emerged as the primary drivers of these effects. These findings underscore the

sensitivity of the early-life period to environmental exposures and suggest that early microbiome–chemical interactions may influence the developmental trajectory of infant metabolism.

A key strength of this study is the use of a well-characterized birth cohort, which allowed us to integrate high-quality exposure data with in-depth metabolomic and microbiome profiling. The comprehensive metabolomic approach employed three LC–MS–based platforms, enabling detection of a wide range of lipid classes, polar metabolites, and microbial-derived compounds. Gut microbiota was assessed using shotgun metagenomics, allowing species-level resolution and functional inference.

We acknowledge some limitations that should be considered when interpreting our findings. The relatively small sample size may limit statistical power and generalizability, and residual confounding cannot be fully excluded despite adjustment for key covariates, including infant sex, breastfeeding status, and mode of delivery. In addition, our study population consisted of infants carrying HLA genotypes associated with increased susceptibility to type 1 diabetes and was recruited from a single clinical site. Thus, this cohort may not fully represent the general population, and the metabolomic and microbiome patterns observed here may have limited generalizability. Although maternal dietary factors correlated with PCB exposure showed minimal associations with the infant metabolome after correction for multiple testing, some degree of residual confounding cannot be ruled out. Nevertheless, our study reports unique and clinically relevant associations between PCB exposure levels and the metabolome and microbiome of the human mother–child dyad at the individual species level that warrants further study.

We also recognize that, while we observed associations among maternal PCB exposure, infant microbial composition, and metabolic alterations particularly involving bile acids, short-chain fatty acids, and other microbially related metabolites these findings are correlational in nature. The cross-sectional study design, together with the absence of causal or mediation modelling and mechanistic in vitro experimentation, precludes strong conclusions regarding cause-and-effect relationships or underlying biological pathways linking PCB exposure, microbiome alterations, and metabolic outcomes. Future studies incorporating larger sample sizes, longitudinal designs, and mechanistic in vitro or experimental approaches will be essential to determine whether specific microbiome changes mediate PCB-associated metabolic effects or represent parallel responses to environmental exposure, and to assess their potential long-term health implications.

CRediT authorship contribution statement

Santosh Lamichhane: Writing – review & editing, Visualization, Methodology, Investigation. **Samira Salihovic:** Writing – review & editing, Methodology, Investigation, Formal analysis. **Tim Sinioja:** Writing – review & editing, Methodology, Investigation. **Suvi M. Virtanen:** Writing – review & editing, Formal analysis. **Tommi Vatanen:** Writing – review & editing, Formal analysis. **Matej Orešič:** Writing – review & editing, Investigation, Formal analysis. **Mikael Knip:** Funding acquisition, Investigation, Resources, Writing – review & editing. **Tuulia Hyötyläinen:** Writing – original draft, Visualization, Supervision, Methodology, Investigation, Formal analysis, Conceptualization.

Funding

This study was supported by the Swedish Research Council (grant no. 2020-03674 and 2016-05176 to T.H and M.O.), Formas (grant no. 2019-00869 to T.H and M.O.), and by the Swedish Knowledge Foundation (grant no. 20220122, to T.H. and M.O.). The EDIA study was supported by the National Institute of Diabetes and Digestive and Kidney Diseases (NIDDK); National Institutes of Health (1DP3DK094338-01); the Academy of Finland Centre of Excellence in Molecular Systems Immunology and Physiology Research 2012-17 (250114); the Medical Research Funds, Tampere and Helsinki University Hospitals. S.L. was supported by Research Council of Finland funding (no. 363417).

Declaration of competing interest

The authors declare that they have no known competing financial interests or personal relationships that could have appeared to influence the work reported in this paper.

Appendix A. Supplementary data

Supplementary data to this article can be found online at https://doi.org/10.1016/j.envint.2026.110080.

Data availability

Data are available upon request and an appropriate institutional collaboration agreement. These data are not available to access in a repository owing to concern that the identity of participants might be revealed inadvertently.

References

Agrawal, M., Midya, V., Maroli, A., Magee, J., Petrick, L., Colombel, J.F., 2024. Per- and poly-fluoroalkyl substances exposure is associated with later occurrence of inflammatory bowel disease. Clin. Gastroenterol. Hepatol. 22 (8), 1728–1730.e1728.

Albillos, A., de Gottardi, A., Rescigno, M., 2020. The gut-liver axis in liver disease: pathophysiological basis for therapy. J. Hepatol. 72 (3), 558–577.

Aminian, O., Moinfar, Z., Eftekhari, S., Esser, A., Schettgen, T., Felten, M., Kaifie, A., Kraus, T., 2020. Association of plasma levels of lipid and polychlorinated biphenyls in Iranian adult. Heliyon 6 (4), e03775.

Ashley-Martin, J., Dodds, L., Arbuckle, T.E., Bouchard, M.F., Fisher, M., Morriset, A.-S., Monnier, P., Shapiro, G.D., Ettinger, A.S., Dallaire, R., Taback, S., Fraser, W., Platt, R.W., 2017. Maternal concentrations of perfluoroalkyl substances and fetal markers of metabolic function and birth weight: the maternal-infant research on environmental chemicals (MIREC) study. Am. J. Epidemiol. 185 (3), 185–193.

Bazarganipour, S., Hausmann, J., Oertel, S., El-Hindi, K., Brachtendorf, S., Blumenstein, I., Kubesch, A., Sprinzl, K., Birod, K., Hahnefeld, L., Trautmann, S., Thomas, D., Herrmann, E., Geisslinger, G., Schiffmann, S., Grösch, S., 2019. The lipid status in patients with ulcerative colitis: sphingolipids are disease-dependent regulated. J. Clin. Med. 8 (7), 971.

Boucher, O., Muckle, G., Bastien, C.H., 2009. Prenatal exposure to polychlorinated biphenyls: a neuropsychologic analysis. Environ. Health Perspect. 117 (1), 7–16.

Caspersen, I.H., Aase, H., Biele, G., Brantsæter, A.L., Haugen, M., Kvalem, H.E., Skogan, A.H., Zeiner, P., Alexander, J., Meltzer, H.M., Knutsen, H.K., 2016. The influence of maternal dietary exposure to dioxins and PCBs during pregnancy on ADHD symptoms and cognitive functions in Norwegian preschool children. Environ. Int. 94, 649–660.

Chen, H., Zhang, W., Sun, X., Zhou, Y., Li, J., Zhao, H., Xia, W., Xu, S., Cai, Z., Li, Y., 2024. Prenatal exposure to multiple environmental chemicals and birth size. J. Expo. Sci. Environ. Epidemiol. 34 (4), 629–636.

Cheng, S.L., Li, X., Lehmler, H.-J., Phillips, B., Shen, D., Cui, J.Y., 2018. Gut microbiota modulates interactions between polychlorinated biphenyls and bile acid homeostasis. Toxicol. Sci. 166 (2), 269–287.

Dean, L.E., Wang, H., Li, X., Fitzjerrells, R.L., Valenzuela, A.E., Neier, K., LaSalle, J.M., Mangalam, A., Lein, P.J., Lehmler, H.J., 2025. Identification of polychlorinated biphenyls (PCBs) and PCB metabolites associated with changes in the gut microbiome of female mice exposed to an environmental PCB mixture. J. Hazard. Mater. 489, 137688.

Dei Cas, M., Paroni, R., Saccardo, A., Casagni, E., Arnoldi, S., Gambaro, V., Saresella, M., Mario, C., La Rosa, F., Marventano, I., Piancone, F., Roda, G., 2020. A straightforward LC-MS/MS analysis to study serum profile of short and medium chain fatty acids. J. Chromatogr. B 1154, 121982.

Donald, K., Serapio-Palacios, A., Bozorgmehr, T., Ma, M., Garcia, M.A.I., Petersen, C., Mandhane, P., Subbarao, P., Moraes, T.J., Simons, E., Turvey, S., Azad, M.B., Finlay, B.B., 2025. Human milk IgA promotes normal immune development by limiting Th17-inducing *Erysipelatoclostridium ramosum* in the infant gut. Proc. Natl. Acad. Sci. 122 (28), e2501030122.

Erkkola, M., Karppinen, M., Javanainen, J., Räsänen, L., Knip, M., Virtanen, S.M., 2001. Validity and reproducibility of a food frequency questionnaire for pregnant Finnish women. Am. J. Epidemiol. 154 (5), 466–476.

Fleisch, A.F., Rifas-Shiman, S.L., Mora, A.M., Calafat, A.M., Ye, X., Luttmann-Gibson, H., Gillman, M.W., Oken, E., Sagiv, S.K., 2017. Early-life exposure to perfluoroalkyl substances and childhood metabolic function. Environ. Health Perspect. 125 (3), 481–487.

Gaggini, M., Ndreu, R., Michelucci, E., Rocchiccioli, S., Vassalle, C., 2022. Ceramides as mediators of oxidative stress and inflammation in cardiometabolic disease. Int. J. Mol. Sci. 23 (5).

Granum, B., Haug, L.S., Namork, E., Stolevik, S.B., Thomsen, C., Aaberge, I.S., van Loveren, H., Lovik, M., Nygaard, U.C., 2013. Pre-natal exposure to perfluoroalkyl

substances may be associated with altered vaccine antibody levels and immune-related health outcomes in early childhood. J. Immunotoxicol. 10 (4), 373–379.
Guzior, D.V., Quinn, R.A., 2021. Review: microbial transformations of human bile acids. Microbiome 9 (1), 140.
Haug, L.S., Huber, S., Becher, G., Thomsen, C., 2011. Characterisation of human exposure pathways to perfluorinated compounds — comparing exposure estimates with biomarkers of exposure. Environ. Int. 37 (4), 687–693.
Haug, L.S., Sakhi, A.K., Cequier, E., Casas, M., Maitre, L., Basagana, X., Andrusaityte, S., Chalkiadaki, G., Chatzi, L., Coen, M., de Bont, J., Dedele, A., Ferrand, J., Grazuleviciene, R., Gonzalez, J.R., Gutzkow, K.B., Keun, H., McEachan, R., Meltzer, H.M., Petraviciene, I., Robinson, O., Saulnier, P.-J., Slama, R., Sunyer, J., Urquiza, J., Vafeiadi, M., Wright, J., Vrijheid, M., Thomsen, C., 2018. In-utero and childhood chemical exposome in six European mother-child cohorts. Environ. Int. 121, 751–763.
Haug, L.S., Thomsen, C., Bechert, G., 2009. Time trends and the influence of age and gender on serum concentrations of perfluorinated compounds in archived human samples. Environ. Sci. Technol. 43.
Hermann, R., Turpeinen, H., Laine, A.P., Veijola, R., Knip, M., Simell, O., Sipilä, I., Åkerblom, H.K., Ilonen, J., 2003. HLA DR-DQ-encoded genetic determinants of childhood-onset type 1 diabetes in Finland: an analysis of 622 nuclear families. Tissue Antigens 62 (2), 162–169.
Hernández-Mesa, M., Narduzzi, L., Ouzia, S., Soetart, N., Jaillardon, L., Guitton, Y., Le Bizec, B., Dervilly, G., 2022. Metabolomics and lipidomics to identify biomarkers of effect related to exposure to non-dioxin-like polychlorinated biphenyls in pigs. Chemosphere 296, 133957.
Hoadley, L., Watters, M., Rogers, R., Siegmann Werner, L., Markiewicz, K.V., Forrester, T., McLanahan, E.D., 2023. Public health evaluation of PFAS exposures and breastfeeding: a systematic literature review. Toxicol. Sci. 194 (2), 121–137.
Hoffman, S.S., Liang, D., Hood, R.B., Tan, Y., Terrell, M.L., Marder, M.E., Barton, H., Pearson, M.A., Walker, D.I., Barr, D.B., Jones, D.P., Marcus, M., 2023. Assessing metabolic differences associated with exposure to polybrominated biphenyl and polychlorinated biphenyls in the michigan PBB registry. Environ. Health Perspect. 131 (10), 107005.
Hou, K., Wu, Z.X., Chen, X.Y., Wang, J.Q., Zhang, D., Xiao, C., Zhu, D., Koya, J.B., Wei, L., Li, J., Chen, Z.S., 2022. Microbiota in health and diseases. Signal Transduct. Target. Ther. 7 (1), 135.
Hyötyläinen, T., McGlinchey, A., Salihovic, S., Schubert, A., Douglas, A., Hay, D.C., O'Shaughnessy, P.J., Iredale, J.P., Shaw, S., Fowler, P.A., Orešič, M., 2024. In utero exposures to perfluoroalkyl substances and the human fetal liver metabolome in Scotland: a cross-sectional study. The Lancet Planetary Health 8 (1), e5–e17.
Kalloo, G., Wellenius, G.A., McCandless, L., Calafat, A.M., Sjodin, A., Romano, M.E., Karagas, M.R., Chen, A., Yolton, K., Lanphear, B.P., Braun, J.M., 2020. Exposures to chemical mixtures during pregnancy and neonatal outcomes: the HOME study. Environ. Int. 134, 105219.
Kim, G., Yoon, Y., Park, J.H., Park, J.W., Noh, M.G., Kim, H., Park, C., Kwon, H., Park, J. H., Kim, Y., Sohn, J., Park, S., Kim, H., Im, S.K., Kim, Y., Chung, H.Y., Nam, M.H., Kwon, J.Y., Kim, I.Y., Kim, Y.J., Baek, J.H., Kim, H.S., Weinstock, G.M., Cho, B., Lee, C., Fang, S., Park, H., Seong, J.K., 2022. Bifidobacterial carbohydrate/nucleoside metabolism enhances oxidative phosphorylation in white adipose tissue to protect against diet-induced obesity. Microbiome 10 (1), 188.
Kim, M.J., Kim, J.E., Lee, M.J., Bae, H.R., Kwon, E.Y., Shin, S.K., 2025. Lactobacillus paragasseri SBT2055 suppressed insulin resistance and fatty liver by inhibiting oxidative stress and inflammation in high-fat diet-induced obese mice. Benef. Microbes 1–14.
Klocke, C., Sethi, S., Lein, P.J., 2020. The developmental neurotoxicity of legacy vs. contemporary polychlorinated biphenyls (PCBs): similarities and differences. Environ. Sci. Pollut. Res. Int. 27 (9), 8885–8896.
Koivusaari, K., Niinistö, S., Nevalainen, J., Honkanen, J., Ruohtula, T., Koreasalo, M., Ahonen, S., Åkerlund, M., Tapanainen, H., Siljander, H., Miettinen, M.E., Alatossava, T., Ilonen, J., Vaarala, O., Knip, M., Virtanen, S.M., 2023. Infant feeding, gut permeability, and gut inflammation markers. J. Pediatr. Gastroenterol. Nutr. 76 (6), 822–829.
Kumar, S., Mukherjee, R., Gaur, P., Leal, É., Lyu, X., Ahmad, S., Puri, P., Chang, C.M., Raj, V.S., Pandey, R.P., 2025. Unveiling roles of beneficial gut bacteria and optimal diets for health. Front. Microbiol. 16, 1527755.
Lamichhane, S., Härkönen, T., Vatanen, T., Hyötyläinen, T., Knip, M., Orešič, M., 2023. Impact of exposure to per- and polyfluoroalkyl substances on fecal microbiota composition in mother-infant dyads. Environ. Int. 176, 107965.
Lamichhane, S., Sen, P., Dickens, A.M., Orešič, M., Bertram, H.C., 2018. Gut metabolome meets microbiome: a methodological perspective to understand the relationship between host and microbe. Methods 149, 3–12.
Lamichhane, S., Siljander, H., Salonen, M., Ruohtula, T., Virtanen, S.M., Ilonen, J., Hyötyläinen, T., Knip, M., Orešič, M., 2022. Impact of extensively hydrolyzed infant formula on circulating lipids during early life. Front. Nutr. 9, 859627.
Lee, Y.J., Jung, H.W., Kim, H.Y., Choi, Y.J., Lee, Y.A., 2021. Early-life exposure to per- and poly-fluorinated alkyl substances and growth, adiposity, and puberty in children: a systematic review. Front. Endocrinol. (Lausanne) 12, 683297.
Lim, J.J., Li, X., Lehmler, H.J., Wang, D., Gu, H., Cui, J.Y., 2020. Gut microbiome critically impacts PCB-induced changes in metabolic fingerprints and the hepatic transcriptome in mice. Toxicol. Sci. 177 (1), 168–187.
Luukkonen, P.K., Zhou, Y., Sadevirta, S., Leivonen, M., Arola, J., Oresic, M., Hyotylainen, T., Yki-Jarvinen, H., 2016. Hepatic ceramides dissociate steatosis and insulin resistance in patients with non-alcoholic fatty liver disease. J. Hepatol. 64 (5), 1167–1175.
McCoin, C.S., Knotts, T.A., Adams, S.H., 2015. Acylcarnitines–old actors auditioning for new roles in metabolic physiology. Nat. Rev. Endocrinol. 11 (10), 617–625.
McGlinchey, A., Sinioja, T., Lamichhane, S., Bodin, J., Siljander, H., Geng, D., Carlsson, C., Duberg, D., Ilonen, J., Virtanen, S.M., Dirven, H., Berntsen, H.F., Zimmer, K., Nygaard, U.C., Orešič, M., Knip, M., Hyötyläinen, T., 2019. prenatal exposure to environmental chemicals modulates serum phospholipids in newborn infants, increasing later risk of type 1 diabetes. bioRxiv(588350): 588350.
McGlinchey, A., Sinioja, T., Lamichhane, S., Sen, P., Bodin, J., Siljander, H., Dickens, A. M., Geng, D., Carlsson, C., Duberg, D., Ilonen, J., Virtanen, S.M., Dirven, H., Berntsen, H.F., Zimmer, K., Nygaard, U.C., Orešič, M., Knip, M., Hyötyläinen, T., 2020. Prenatal exposure to perfluoroalkyl substances modulates neonatal serum phospholipids, increasing risk of type 1 diabetes. Environ. Int. 143, 105935.
Mihalik, S.J., Goodpaster, B.H., Kelley, D.E., Chace, D.H., Vockley, J., Toledo, F.G., DeLany, J.P., 2010. Increased levels of plasma acylcarnitines in obesity and type 2 diabetes and identification of a marker of glucolipotoxicity. Obesity (Silver Spring) 18 (9), 1695–1700.
Ouidir, M., Mendola, P., Buck Louis, G.M., Kannan, K., Zhang, C., Tekola-Ayele, F., 2020. Concentrations of persistent organic pollutants in maternal plasma and epigenome-wide placental DNA methylation. Clin. Epigenetics 12 (1), 103.
Pan, Y., Li, J., Lin, P., Wan, L., Qu, Y., Cao, L., Wang, L., 2024. A review of the mechanisms of abnormal ceramide metabolism in type 2 diabetes mellitus, Alzheimer's disease, and their co-morbidities. Front. Pharmacol. 15, 1348410.
Pang, Z., Lu, Y., Zhou, G., Hui, F., Xu, L., Viau, C., Spigelman, A.F., MacDonald, P.E., Wishart, D.S., Li, S., Xia, J., 2024. MetaboAnalyst 6.0: towards a unified platform for metabolomics data processing, analysis and interpretation. Nucleic Acids Res. 52 (W1), W398–W406.
Peng, Y., Zhu, J., Wang, S., Liu, Y., Liu, X., DeLeon, O., Zhu, W., Xu, Z., Zhang, X., Zhao, S., Liang, S., Li, H., Ho, B., Ching, J.-Y.-L., Cheung, C.P., Leung, T.F., Tam, W. H., Leung, T.Y., Chang, E.B., Chan, F.K.L., Zhang, L., Ng, S.C., Tun, H.M., 2024. A metagenome-assembled genome inventory for children reveals early-life gut bacteriome and virome dynamics. Cell Host Microbe 32 (12), 2212–2230.e2218.
Pluskal, T., Castillo, S., Villar-Briones, A., Oresic, M., 2010. MZmine 2: modular framework for processing, visualizing, and analyzing mass spectrometry-based molecular profile data. BMC Bioinf. 11, 395.
Roszczyc-Owsiejczuk, K., Zabielski, P., 2021. Sphingolipids as a culprit of mitochondrial dysfunction in insulin resistance and type 2 diabetes, Front. Endocrinol., 12.
Salihovic, S., Mattioli, L., Lindström, G., Lind, L., Lind, P.M., van Bavel, B., 2012. A rapid method for screening of the Stockholm Convention POPs in small amounts of human plasma using SPE and HRGC/HRMS. Chemosphere 86 (7), 747–753.
Sen, P., Qadri, S., Luukkonen, P.K., Ragnarsdottir, O., McGlinchey, A., Jäntti, S., Juuti, A., Arola, J., Schlezinger, J.J., Webster, T.F., Orešič, M., Yki-Järvinen, H., Hyötyläinen, T., 2022. Exposure to environmental contaminants is associated with altered hepatic lipid metabolism in non-alcoholic fatty liver disease. J. Hepatol. 76 (2), 283–293.
Shi, X., Wahlang, B., Wei, X., Yin, X., Falkner, K.C., Prough, R.A., Kim, S.H., Mueller, E. G., McClain, C.J., Cave, M., Zhang, X., 2012. Metabolomic analysis of the effects of polychlorinated biphenyls in nonalcoholic fatty liver disease. J. Proteome Res. 11 (7), 3805–3815.
Siljander, H., Jason, E., Ruohtula, T., Selvenius, J., Koivusaari, K., Salonen, M., Ahonen, S., Honkanen, J., Ilonen, J., Vaarala, O., Virtanen, S.M., Lähdeaho, M.-L., Knip, M., 2021. Effect of early feeding on intestinal permeability and inflammation markers in infants with genetic susceptibility to type 1 diabetes: a randomized clinical trial. J. Pediatr. 238, 305–311.e303.
Sinisalu, L., Sen, P., Salihovic, S., Virtanen, S., Hyoty, H., Ilonen, J., Toppari, J., Veijola, R., Oresic, M., Knip, M., Hyotylainen, T., 2020. Early-life exposure to perfluorinated alkyl substances modulates lipid metabolism in progression to celiac disease, 2020.2004.2002.20051359.
Starling, A.P., Adgate, J.L., Hamman, R.F., Kechris, K., Calafat, A.M., Dabelea, D., 2019. Prenatal exposure to per- and polyfluoroalkyl substances and infant growth and adiposity: the healthy start study. Environ. Int. 131, 104983.
Starling, A.P., Adgate, J.L., Hamman, R.F., Kechris, K., Calafat, A.M., Ye, X., Dabelea, D., 2017. Perfluoroalkyl substances during pregnancy and offspring weight and adiposity at birth: examining mediation by maternal fasting glucose in the healthy start study. Environ. Health Perspect. 125 (6), 067016.
Stratakis, N., Rock, S., La Merrill, M.A., Saez, M., Robinson, O., Fecht, D., Vrijheid, M., Valvi, D., Conti, D.V., McConnell, R., Chatzi, V.L., 2022. Prenatal exposure to persistent organic pollutants and childhood obesity: a systematic review and meta-analysis of human studies. Obes. Rev. 23 (Suppl 1), e13383.
Stubleski, J., Kukucka, P., Salihovic, S., Lind, P.M., Lind, L., Kärrman, A., 2018. A method for analysis of marker persistent organic pollutants in low-volume plasma and serum samples using 96-well plate solid phase extraction. J. Chromatogr. A 1546, 18–27.
Takagaki, A., Nanjo, F., 2016. Biotransformation of (-)-epicatechin, (+)-epicatechin, (-)-catechin, and (+)-catechin by intestinal bacteria involved in isoflavone metabolism. Biosci. Biotechnol. Biochem. 80 (1), 199–202.
Tamayo-Uria, I., Maitre, L., Thomsen, C., Nieuwenhuijsen, M.J., Chatzi, L., Siroux, V., Aasvang, G.M., Agier, L., Andrusaityte, S., Casas, M., de Castro, M., Dedele, A., Haug, L.S., Heude, B., Grazuleviciene, R., Gutzkow, K.B., Krog, N.H., Mason, D., McEachan, R.R.C., Meltzer, H.M., Petraviciene, I., Robinson, O., Roumeliotaki, T., Sakhi, A.K., Urquiza, J., Vafeiadi, M., Waiblinger, D., Warembourg, C., Wright, J., Slama, R., Vrijheid, M., Basagaña, X., 2019. The early-life exposome: description and patterns in six European countries. Environ. Int. 123, 189–200.
Tang-Péronard, J.L., Heitmann, B.L., Andersen, H.R., Steuerwald, U., Grandjean, P., Weihe, P., Jensen, T.K., 2014. Association between prenatal polychlorinated biphenyl exposure and obesity development at ages 5 and 7 y: a prospective cohort study of 656 children from the Faroe Islands. Am. J. Clin. Nutr. 99 (1), 5–13.
Team, R.C., 2017. R: A Language and Environment for Statistical Computing, R Foundation for Statistical Computing, Vienna, Austria.

Tian, Y., Gui, W., Rimal, B., Koo, I., Smith, P.B., Nichols, R.G., Cai, J., Liu, Q., Patterson, A.D., 2020. Metabolic impact of persistent organic pollutants on gut microbiota. Gut Microbes 12 (1), 1–16.

Tian, Y., Rimal, B., Gui, W., Koo, I., Yokoyama, S., Perdew, G.H., Patterson, A.D., 2022. Early life short-term exposure to polychlorinated biphenyl 126 in mice leads to metabolic dysfunction and microbiota changes in adulthood. Int. J. Mol. Sci. 23 (15).

Tito Damiani A, , Aleksandr Smirnov, S.H., Mokshyna, O., Brungs, C., Korf, A., Smith, J., Stincone, P., Dreolin Author, N., Nothias, L.-F., Hyötyläinen, T., Orešič , M., Karst, U., Dorrestein, P., Petras, D., Du, X., van der Hooft, J., Schmid, R., Pluskal, T., 2024. Reproducible mass spectrometry data processing and compound annotation in MZmine 3, Chemrxiv.

Vafeiadi, M., Georgiou, V., Chalkiadaki, G., Rantakokko, P., Kiviranta, H., Karachaliou, M., Fthenou, E., Venihaki, M., Sarri, K., Vassilaki, M., Kyrtopoulos, S. A., Oken, E., Kogevinas, M., Chatzi, L., 2015. Association of prenatal exposure to persistent organic pollutants with obesity and cardiometabolic traits in early childhood: the rhea mother-child cohort (Crete, Greece). Environ. Health Perspect. 123 (10), 1015–1021.

Vatanen, T., Jabbar, K.S., Ruohtula, T., Honkanen, J., Avila-Pacheco, J., Siljander, H., Stražar, M., Oikarinen, S., Hyöty, H., Ilonen, J., Mitchell, C.M., Yassour, M., Virtanen, S.M., Clish, C.B., Plichta, D.R., Vlamakis, H., Knip, M., Xavier, R.J., 2022. Mobile genetic elements from the maternal microbiome shape infant gut microbial assembly and metabolism. Cell 185 (26), 4921–4936.e4915.

Verhulst, S.L., Nelen, V., Hond, E.D., Koppen, G., Beunckens, C., Vael, C., Schoeters, G., Desager, K., 2009. Intrauterine exposure to environmental pollutants and body mass index during the first 3 years of life. Environ. Health Perspect. 117 (1), 122–126.

Wang, Q., Chen, B., Sheng, D., Yang, J., Fu, S., Wang, J., Zhao, C., Wang, Y., Gai, X., Wang, J., Stirling, K., Heng, X., Man, H., Zhang, L., 2022. Multiomics analysis reveals aberrant metabolism and immunity linked gut microbiota with insomnia. Microbiol Spectr 10 (5), e0099822.

Wilson, R.J., Suh, Y.P., Dursun, I., Li, X., da Costa Souza, F., Grodzki, A.C., Cui, J.Y., Lehmler, H.J., Lein, P.J., 2024. Developmental exposure to the Fox River PCB mixture modulates behavior in juvenile mice. Neurotoxicology 103, 146–161.

Woods, M.M., Lanphear, B.P., Braun, J.M., McCandless, L.C., 2017. Gestational exposure to endocrine disrupting chemicals in relation to infant birth weight: a Bayesian analysis of the HOME Study. Environ. Health 16 (1), 115.

Woting, A., Pfeiffer, N., Loh, G., Klaus, S., Blaut, M., 2014. *Clostridium ramosum* promotes high-fat diet-induced obesity in gnotobiotic mouse models. MBio 5 (5), e01530–01514.

Wu, J., Li, M., Zhou, C., Rong, J., Zhang, F., Wen, Y., Qu, J., Wu, R., Miao, Y., Niu, J., 2024. Changes in amino acid concentrations and the gut microbiota composition are implicated in the mucosal healing of ulcerative colitis and can be used as noninvasive diagnostic biomarkers. Clin. Proteomics 21 (1), 62.

Yao, C., Li, X., Tang, M., Liu, L., Cai, X., Yuan, X., Hu, J., Zhao, J., Qiao, W., Zhang, Y., Chen, L., 2025. Lactobacillus paragasseri HM018 derived from breast milk ameliorates hyperlipidemia in high-cholesterol rats by modulating bile acid metabolism. Front. Microbiol. 16, 1599931.

Zhou, Y., Hu, L.-W., Qian, Z., Geiger, S.D., Parrish, K.L., Dharmage, S.C., Campbell, B., Roponen, M., Jalava, P., Hirvonen, M.-R., Heinrich, J., Zeng, X.-W., Yang, B.-Y., Qin, X.-D., Lee, Y.L., Dong, G.-H., 2017. Interaction effects of polyfluoroalkyl substances and sex steroid hormones on asthma among children. Sci. Rep. 7 (1), 899.